Hypoxia Increases Cytosolic Ca^{2+} In Goldfish Horizontal Cells Exposed to Glutamate

Nicole Nagy

Thesis submitted to the University of Ottawa
in partial Fulfillment of the requirements for the
Master's degree in biology

Department of Biology
Faculty of Science
University of Ottawa

ACKNOLEDGEMENTS

I would like to acknowledge that doing an MSc during COVID was probably not a good idea.

First and foremost, thanks go out to Dr. Michael Jonz, who is a very patient supervisor. Thanks to Dr. John Lewis and Dr. Matthew Pamenter for serving as members of my thesis advisory committee and to Dr. Michael Country for the time he spent training me in the lab.

Finally, thank you to Matthew Watson.

ABSTRACT

Central neurons of the common goldfish (*Carassius auratus*) are exceptional in their capacity to survive Ca^{2+}-induced excitotoxicity and cell death during hypoxia. Horizontal cells (HCs) are inhibitory interneurons of the retina that are tonically depolarized by the neurotransmitter, glutamate, yet preserve intracellular Ca^{2+} homeostasis. In HCs isolated from goldfish, and in the absence of glutamatergic input, intracellular Ca^{2+} concentration ($[Ca^{2+}]_i$) is protected from prolonged exposure to hypoxia by mitochondrial ATP-dependent K^+ (mK_{ATP}) channel activity. In the present study, we investigated the effects of hypoxia upon $[Ca^{2+}]_i$ in isolated HCs during tonic activation by glutamate to better predict the effects of hypoxia in the active retina. Dynamic changes in $[Ca^{2+}]_i$ were measured using the ratiometric Ca^{2+} indicator, Fura-2. Application of 100 μM glutamate during hypoxia (P_{O2} = 25 mmHg) produced a greater rise in $[Ca^{2+}]_i$ compared to the same glutamate stimulus during normoxia. The hypoxia-dependent increase in $[Ca^{2+}]_i$ was abolished by application of 5-hydroxydecanoic acid, which renders mK_{ATP} channels inactive. Extracellular Ca^{2+} did not contribute to the elevated $[Ca^{2+}]_i$ observed during hypoxia, as the effect persisted in Ca^{2+}-free solution and during application of verapamil, an L-type Ca^{2+} channel blocker. By contrast, inhibition of the mitochondrial Ca^{2+} uniporter or ryanodine receptors (with ruthenium red or ryanodine, respectively) abolished the hypoxia-dependent rise in $[Ca^{2+}]_i$. This study reports a paradoxical mK_{ATP}-dependent rise in $[Ca^{2+}]_i$ during hypoxia in HCs activated by glutamate, and suggests roles for the mitochondria and intracellular Ca^{2+} stores in regulating this mechanism.

RÉSUMÉ

Les neurones centraux du poisson rouge commun (*Carassius auratus*) sont exceptionnels dans leur capacité à survivre à l'excitotoxicité induite par le Ca^{2+} et à la mort cellulaire pendant l'hypoxie. Les cellules horizontales (CH) sont des interneurones inhibiteurs de la rétine qui sont à la fois dépolarisées de manière tonique par le neurotransmetteur, le glutamate, tout en préservant l'homéostasie intracellulaire du Ca^{2+}. Dans les CH isolées du poisson rouge, et en l'absence d'entrée glutamatergique, la concentration intracellulaire en Ca^{2+} ($[Ca^{2+}]_i$) est protégée d'une exposition prolongée à l'hypoxie grâce à l'activité des canaux K^+ mitochondriaux dépendant de l'ATP (mK_{ATP}). Dans cette étude, nous avons étudié les effets de l'hypoxie sur $[Ca^{2+}]_i$ dans des CH isolées pendant l'activation tonique par le glutamate afin de mieux prédire les effets de l'hypoxie dans la rétine active. Des changements dynamiques dans $[Ca^{2+}]_i$ ont été mesurés à l'aide de l'indicateur de Ca^{2+} par rapport, Fura-2. L'application de 100 µM de glutamate pendant l'hypoxie (P_{O2} = 25 mmHg) a produit une augmentation plus importante de $[Ca^{2+}]_i$ par rapport au même stimulus de glutamate pendant la normoxie. L'augmentation de $[Ca^{2+}]_i$ dépendante de l'hypoxie a été abolie par l'application d'acide 5-hydroxydécanoïque, qui rend les canaux mK_{ATP} inactifs. Le Ca^{2+} extracellulaire n'a pas contribué à l'élévation de $[Ca^{2+}]_i$ observée pendant l'hypoxie, car l'effet a persisté dans une solution sans Ca^{2+} et pendant l'application de vérapamil, un bloqueur des canaux Ca^{2+} de « L-type ». En revanche, l'inhibition du transporteur uniporteur de Ca^{2+} mitochondrial ou des récepteurs à la ryanodine (avec du rouge de ruthénium ou de la ryanodine, respectivement) a aboli l'augmentation de $[Ca^{2+}]_i$ dépendante de l'hypoxie. Cette étude rapporte une augmentation paradoxale de $[Ca^{2+}]_i$ dépendante des mK_{ATP} pendant l'hypoxie dans des CH activées par le glutamate, et suggère des rôles pour les mitochondries et les réserves intracellulaires de Ca^{2+} dans la régulation de ce mécanisme.

TABLE OF CONTENTS

LIST OF FIGURES & TABLES

LIST OF ABBREVIATIONS AND UNITS

ABBREVIATIONS

$[Ca^{2+}]$	Concentration of calcium ion
$[Ca^{2+}]_i$	Intracellular concentration of calcium ions
°C	Degrees Celsius
µM	Micromolar
µm	Micron
5-HD	5-hydroxydecanoate
AMPAR	α-amino-3-hydroxy-5-methyl-4-isoxazolepropionic acid receptor
ATP	Adenosine triphosphate
Ca^{2+}_e	Extracellular Ca^{2+}
CICR	Ca^{2+}-induced Ca^{2+} release
CNS	Central nervous system
DMSO	Dimethyl sulfoxide
ECS	Extracellular solution
ER	Endoplasmic reticulum
Fura-2-AM	Fura-2-acetoxymethyl ester
g	Grams
GABA	γ-aminobutyric acid
$GABA_C$	γ-aminobutyric acid-gated Cl^- channel
h	Hours
HC	Horizontal cell

HEPES	4-(2-hydroxyethyl)-1-piperazineethanesulfonic acid
iGluR	Ionotropic glutamate receptor
L-15	Leibovitz's medium
MCU	Mitochondrial Ca^{2+} uniporter
mGluRs	Metabotropic glutamate receptors
min	Minutes
mK_{ATP}	Mitochondrial adenosine triphosphate-dependent potassium channel
ml	Milliliter
mM	Millimolar
mm	Millimeter
mmHg	Millimeters of mercury
nM	Nanomolar
nm	Nanometer
NMDAR	*N*-methyl-D-aspartate receptor
N_2	Nitrogen
pH	Potential of hydrogen
PMCA	Plasma membrane Ca^{2+}-ATPase
P_{O2}	Partial pressure of oxygen
$R_{340/380}$	Ratio of fluorescence from 340 nm excitation over 380 nm excitation
ROS	Reactive oxygen species
s	Second
SD	Standard deviation
SERCA	Sarcoplasmic/endoplasmic reticulum Ca^{2+} ATPase

U	Units
UV	Ultraviolet
VGCC	Voltage-gated Ca^{2+} channel
v/v	Volume by volume

1. INTRODUCTION

1.1 General Introduction

Oxygen is essential for vertebrate life. Insufficient oxygen availability (hypoxia) or the absence of oxygen (anoxia) often causes severe physiological consequences including cellular dysfunction, metabolic disturbances, and eventually irreversible cellular injury and death. Hypoxia, anoxia, and ischemia (reduced blood flow) can provoke pathophysiological changes and contribute to various diseases including pulmonary hypertension, myocardial infarction, stroke, and diabetic retinopathy. Understanding the mechanisms and consequences of these oxygen-related conditions is critical for the development of therapeutic strategies aimed at mitigating their effects. Insufficient oxygen hinders oxidative phosphorylation and forces cells to shift towards anerobic respiration, leading to significantly lower adenosine triphosphate (ATP) production and the accumulation of toxic lactic acid produced through the fermentation of glucose. In neurons, which possess high ATP demands associated with maintaining transmembrane ion gradients, hypoxia is especially threatening. Failure to maintain these gradients leads to cellular depolarization and the influx of calcium ions (Ca^{2+}) which trigger the onset of "excitotoxic cell death". Some species, such as Crucian carp (*Carassius carassius*), the congeneric goldfish (*Carassius auratus*) and certain freshwater turtles have developed neuroprotective strategies within the central nervous system (CNS) to tolerate prolonged periods of hypoxia or anoxia.

As will be described in the following sections, most studies on hypoxia tolerance in these species have been focused on the brain. By contrast, our understanding of hypoxia tolerance in the retina—a part of the CNS—is only now beginning to emerge. Within the retina,

photoreceptors translate light signals into the excitatory neurotransmitter glutamate. Horizontal cells (HCs) modulate this signal through an inhibitory feedback loop called lateral inhibition. Despite being chronically depolarized by continuous exposure to glutamate, HCs are resistant to excitotoxic cell death.

This thesis examined how intracellular Ca^{2+} concentrations ($[Ca^{2+}]_i$) in goldfish HCs during glutamate responses were impacted by hypoxia. The current introduction will provide background on excitotoxic cell death and hypoxia tolerance as well as HCs and their role within the vertebrate retina. The introduction concludes by outlining the research objectives of this thesis.

1.2 Hypoxia

This section will review how hypoxia initiates cellular processes responsible for excitotoxic cell death. Drawing from examples of hypoxia tolerance in vertebrates, this section will also outline some of the metabolic and neuronal strategies used by these species to survive prolonged exposure to hypoxia/anoxia.

1.2.1 Excitotoxic cell death

ATP is the primary energy molecule of life and is most efficiently manufactured though aerobic respiration via oxidative phosphorylation by the mitochondria. In the absence of sufficient oxygen, cells must shift to anaerobic respiration where ATP is produced at a tenth the efficiency through the fermentation of pyruvate from glucose. Neurons of the CNS, including

those of the retina, may consume up to 50% of cellular energy stores in order to maintain activity of ATP-dependent pumps, which transport ions across the plasma membrane, contribute to maintaining electrical membrane potential and maintain low $[Ca^{2+}]_i$ (Ames, 1992; Erecińska and Silver, 1994; Nilsson and Lutz, 2004). When ATP supply is diminished, such as during periods of hypoxia or ischemia, neurons undergo a cascade of events, including membrane depolarization, activation of voltage-gated Ca^{2+} channels (VGCCs), subsequent elevation of $[Ca^{2+}]_i$, and these may go on to initiate excessive release of excitatory neurotransmitter glutamate into the extracellular space (Bickler and Buck, 1998; Szydlowska and Tymianski, 2010). Glutamate binds three major families of ionotropic glutamate receptors (iGluRs): N-methyl-D-aspartate receptors (NMDARs), α-amino-3-hydroxy-5-methyl-4-isoxazolepropionic acid receptors (AMPARs) and kainate receptors (Watkins et al., 1990; Watkins and Olverman, 1987). All NMDARs, and a subset of AMPARs and kainate receptors, are highly Ca^{2+} permeable (MacDermott et al., 1986); overactivation of iGluRs triggers rapid and widespread Ca^{2+}-dependant cell death (Choi et al., 1988; Frandsen and Schousboe, 1991; Kim et al., 1987; Koh et al., 1990). The sustained elevation of $[Ca^{2+}]_i$ produces free radicals and activates endonucleases, proteases, and phospholipases associated with breaking down the cell in a pathway that is collectively referred to as excitotoxic cell death (Chan et al., 1985; Choi, 1990; Dykens et al., 1987; Siman et al., 1989).

1.2.2 Hypoxia tolerance

Some species have evolved neuroprotective strategies to avoid excitotoxic cell death during hypoxic and anoxic insult. Crucian carp are champions of hypoxia tolerance and can

survive for months in hypoxia at low temperatures (Holopainen and Pitkänen, 1985; Nilsson and Lutz, 2004). The closely related congeneric goldfish can survive for days at 4ºC and hours at room temperature (Walker and Johansen, 1977a; Wilkie et al., 2008). In the absence of oxygen, these two species mobilize large reserves of glycogen to produce energy (Hyvärinen et al., 1985; Nilsson, 1990; Walker and Johansen, 1977b). These species sidestep lactic acidosis by converting the resulting lactate into ethanol and CO_2 which diffuse out through the gills (Shoubridge and Hochachka, 1980). To conserve glycogen stores, *Carassius* spp. suppress their metabolism to approximately a third its normal capacity (van Waversveld et al., 1989). During this time, they maintain a reduced level of locomotion and neural activity (Nilsson et al., 1993). Within the CNS, hypoxia strongly suppresses activity of the auditory nerve in goldfish and eliminates evoked potentials in the retina and optic tectum of crucian carp (Johansson et al., 1997; Suzue et al., 1987). In both cases, the deafness and blindness observed during hypoxia reverse following normoxic reperfusion. The mechanisms responsible for orchestrating the suppression and restoration of these sensory pathways in *Carassius* remain unclear.

Certain freshwater turtles such as the painted turtle (*Chrysemys picta*) and the red-eared slider (*Trachemys scripta*) are also able to spend months in anoxic waters as they overwinter under ice (Herbert and Jackson, 1985; Ultsch and Jackson, 1982). Unlike *Carassius*, which remain active during hypoxia, turtles reduce metabolism to approximately a tenth of their aerobic level and enter a comatose-like state (Herbert and Jackson, 1985). During this time, red-eared sliders show an 80% decrease in heart rate and cardiac output, near complete suppression of electroencephalogram activity, and a 70% - 80% reduction in brain ATP turnover in the brain (estimated based on lactate production) (Fernandes et al., 1997; Hicks and Farrell, 2000; Lutz et al., 1984).

Within the anoxia-tolerant turtle brain, ion channels including in K^+ channels (Pek-Scott and Lutz, 1998; Rodgers-Garlick et al., 2013), Na^+ channels (Perez-Pinzon et al., 1992), AMPARs and NMDARs (Buck and Bickler, 1998; Pamenter et al., 2008a, 2008b; Zivkovic and Buck, 2010) undergo "channel arrest". Channel arrest is the downregulation of ion channels to reduce membrane excitability during cellular stress (Hochachka, 1986) and is also observed in NMDARs in the goldfish telencephalon (Wilkie et al., 2008). In the context of hypoxia/anoxia tolerance, this strategy offers two major neuroprotective benefits: 1) increased membrane stability reduces ATP turnover for ion gradient maintenance, thus conserving energy, and 2) decreased activation of excitatory glutamatergic AMPARs and NMDARs reduces Ca^{2+} entry associated with excitotoxic cell death. The pathway linking the onset of anoxia to suppression of NMDAR and AMPAR currents in turtles is attributed to second messenger effects caused by a subtle "paradoxical" increase in cytosolic [Ca^{2+}] following activation of mitochondria ATP-sensitive K^+ (mK_{ATP}) channels (Pamenter et al., 2008a, 2008b; Zivkovic and Buck, 2010).

1.2.3 mK_{ATP} channels

mK_{ATP} channels are located on the mitochondrial inner membrane and play a central role in ischemic preconditioning, where they confer protective benefits against subsequent hypoxic/anoxic insult across a broad range of species and tissues (Hanley and Daut, 2005; Minners et al., 2003). Although the precise activation mechanism behind these channels is unclear, it's generally supposed that mK_{ATP} channels open in response to decreases in ATP concentration associated with reduced oxidative phosphorylation during hypoxia. Active mK_{ATP} channels facilitate K^+ influx to the mitochondrial matrix which is counteracted by the K^+/H^+

exchanger, disrupting the H^+ gradient, and uncoupling mitochondria (Garlid and Paucek, 2003). Thus, mK_{ATP} channel activation affects membrane potential-dependant mitochondrial functions including ATP synthesis, mitochondrial Ca^{2+} transport, and production of reactive oxygen species (ROS).

In cortical neurons of the painted turtle, mK_{ATP}-mediated mitochondrial depolarization causes the mitochondrial permeability transition pore to release a sub-lethal quantity of Ca^{2+} into the cytosol, subtly elevating baseline $[Ca^{2+}]_i$ levels (Hawrysh and Buck, 2013; Pamenter et al., 2008b; Zivkovic and Buck, 2010). This "paradoxical increase" in $[Ca^{2+}]_i$ activates second messenger pathways that downregulate AMPARs (Pamenter et al., 2008a; Zivkovic and Buck, 2010), NMDARs (Pamenter et al., 2008b; Shin et al., 2005), and Ca^{2+}-dependant K^+ channels (Rodgers-Garlick et al., 2013), ultimately reducing excitability of the neuron and decreasing the occurrence of larger Ca^{2+} influxes associated with excitotoxic cell death.

Interestingly, this signalling mechanism does not appear to extend to goldfish HCs. While turtle cortical neurons display an mK_{ATP}-mediated increase in $[Ca^{2+}]_i$ upon hypoxic perfusion (Hawrysh and Buck, 2013; Pamenter et al., 2008b), isolated goldfish HCs in the absence of glutamate maintain baseline $[Ca^{2+}]_i$ and resist increases during hypoxia as a function of mK_{ATP} activation (Country and Jonz, 2021). Furthermore, pharmacological activation of mK_{ATP} channels via application of diazoxide in the otherwise hypoxia-*intolerant* HCs of rainbow trout (*Oncorhynchus mykiss*) produced $[Ca^{2+}]_i$ stabilizing effects against hypoxia similar to those observed in goldfish (Country and Jonz, 2021). Although mK_{ATP} channels induce neuroprotection against hypoxia in both turtle cortical neurons and goldfish HCs, the pathways responsible for conferring these neuroprotective effects likely differ.

1.3 The retina

The retina is an extension of the brain that lines the back of the eye. This stratified piece of neural tissue is responsible for converting light stimuli from the external environment into neural signals through phototransduction. These electrical stimuli are then transmitted across the distinct strata of retinal neurons where the first steps in visual processing occur prior to being relayed to the optic tectum in the brain. The retina's separation from the rest of the brain, physiologically distinctive cell types, and highly conserved organization led to it being dubbed an "accessible part of the brain" (Dowling, 1987). As such, the retina has been researched extensively across species for over a century, not only for its role in vision but also as a model for neuronal signalling in the CNS (Ramón y Cajal, 1909).

The vertebrate retina is organized into three distinct nuclear layers: the outer nuclear layer, inner nuclear layer, and ganglion cell layer. These contain the cell bodies of photoreceptors, bipolar cells and ganglion cells, respectively (Fig. 1). These cells form a vertical pathway mediated by excitatory, glutamatergic interactions that are ultimately transmitted to the brain via the optic nerve. The inner nuclear layer also contains the cell bodies of laterally-transmitting HCs and amacrine cells. These cells mediate the horizontal inhibitory pathway in synaptically dense regions of neuronal processes, called plexiform layers.

HC interactions occur in the outer plexiform layer (between the inner and outer nuclear layers), where they modulate synaptic activity between photoreceptors and bipolar cells (Thoreson and Mangel, 2012). Similarly, amacrine cell processes extend to the inner plexiform layer (between the outer nuclear and ganglion cell layers), where they influence the synaptic interactions between bipolar and ganglion cells. Both HCs and amacrine cells form sprawling lateral networks to modulate signaling between multiple neighbouring synapses. The resulting

signal is finally received by the ganglion cells whose axons come together to form the optic nerve which carries the information out of the eye and towards the brain.

Figure 1. Schematic representation of the vertebrate retina, illustrating its distinct layers and cell types. Light is absorbed by the outer segments of rod and cone photoreceptors in the outer nuclear layer, where phototransduction is then carried out. The pigment epithelium absorbs scattered light and plays a supportive role in photoreceptor function. The signal produced by phototransduction is transmitted to bipolar cells and horizontal cells at synapses in the outer plexiform layer. Horizontal cell, bipolar cell, and amacrine cell bodies are all located in the inner nuclear layer. Bipolar cells synapse with amacrine cells and ganglion cells at the inner plexiform layer. Finally, the signal is received by ganglion cells and is relayed to the brain via their axons which join to form the optic nerve. Illustration created in BioRender.com

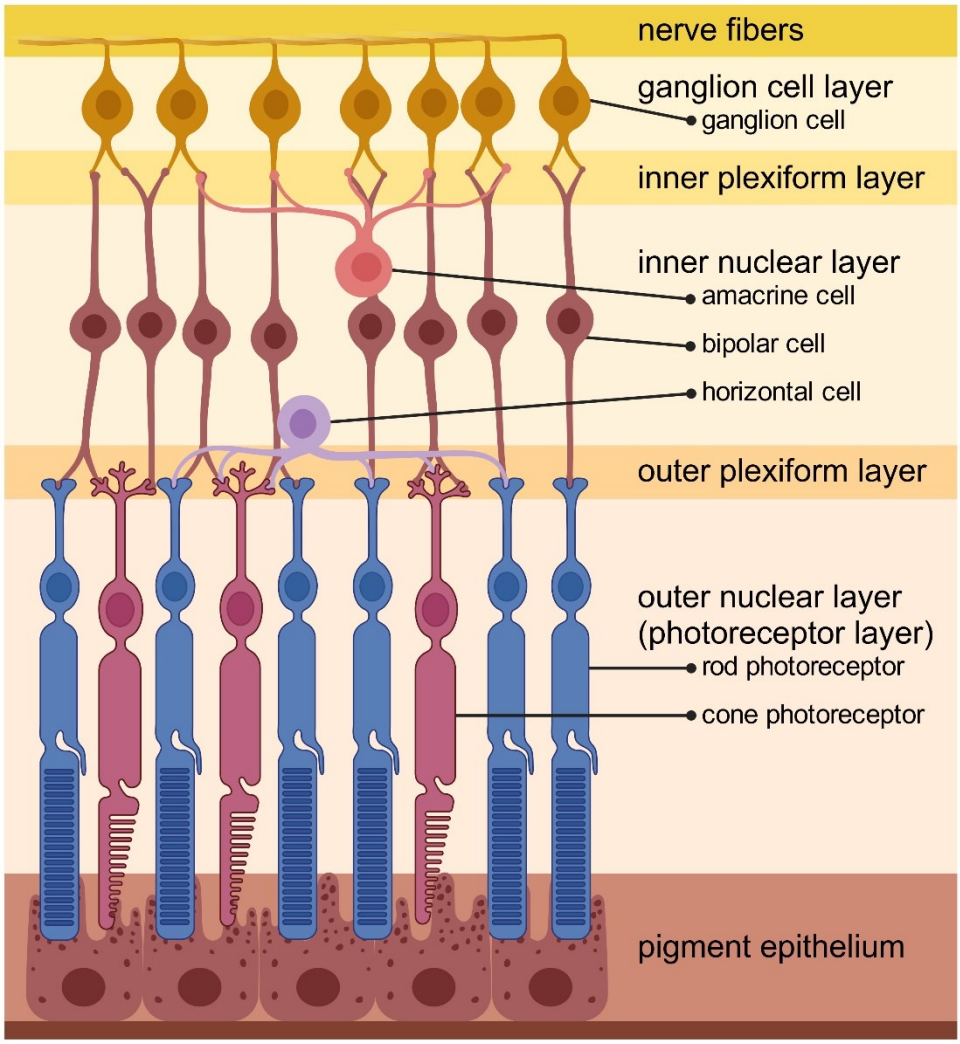
nerve fibers
ganglion cell layer
ganglion cell
inner plexiform layer
inner nuclear layer
amacrine cell
bipolar cell
horizontal cell
outer plexiform layer
outer nuclear layer
(photoreceptor layer)
rod photoreceptor
cone photoreceptor
pigment epithelium

Figure 1

1.3.1 Photoreceptors and phototransduction

Photoreceptors are the first neurons in the visual signalling pathway (Fig. 1). These cells convert light stimuli into neural signals via phototransduction. There are the two main types of photoreceptors: rods and cones. Rods are sensitive to low light levels and facilitate vision in dim light environments, whereas cones are responsible for color vision and function optimally in bright settings (Dowling, 1987).

Photoreceptors synapse with postsynaptic bipolar cells and HCs. Anchored to the presynaptic membrane are electron dense ribbon structures with hundreds of glutamate-filled synaptic vesicles that rapidly fuse with the plasma membrane, releasing excitatory glutamate into the postsynaptic cleft (Heidelberger et al., 2005; Sterling and Matthews, 2005). Vesicular glutamate release is Ca^{2+}-dependant and classically involves a depolarization-induced Ca^{2+} influx followed by Ca^{2+}-induced Ca^{2+} release (CICR) from intracellular stores (Suryanarayanan and Slaughter, 2006). In darkness, photoreceptors are depolarized to approximately –40 mV, L-type VGCCs are active, and the resulting Ca^{2+} influx promotes a continuous release of glutamate to the cleft (Dowling and Ripps, 1973; Schmitz and Witkovsky, 1997; Witkovsky et al., 1997).

Phototransduction allows photoreceptors to encode light intensity by modulating the rate at which glutamate is tonically released from the presynaptic terminal. When light stimulates the pigment molecule retinal, it initiates a biochemical cascade that produces a graded hyperpolarizing effect at the presynaptic membrane and restricts neurotransmitter release into the synaptic cleft (Witkovsky et al., 1997). Importantly, this means that light stimulation *reduces* the release of excitatory glutamate into the cleft and inhibits activation of postsynaptic HCs and bipolar cells

1.3.2 Horizontal cells

HCs are inhibitory interneurons that contribute to the perception of visual contrast though edge detection and colour opponency (Thoreson and Mangel, 2012; Twig et al., 2003). These cells have a distinctive stellate morphology with large flat somas and thick dendrites, making them easy to discern from other retinal cell types (Dowling et al., 1985; Tachibana, 1981). In the teleost fish retina, HCs are especially large and clearly organized in layers according to subtype (Stell and Lightfoot, 1975). As such, teleost HCs are a convenient model neuron that are well suited for intracellular recordings and have been studied extensively for decades (Dowling, 1987).

In darkness, glutamate is released from the photoreceptor terminal onto postsynaptic HC and bipolar cell processes. HCs respond to glutamate with graded changes in membrane potential which allows them to encode signal intensity (Baylor et al., 1971; Svaetichin and MacNichol Jr, 1958; Verweij et al., 1996). Unlike bipolar cells, which synapses with just a single photoreceptor, HCs synapse with multiple nearby photoreceptors. They then integrate the excitatory inputs of these neighbouring photoreceptors and produce an inhibitory signal that downregulates glutamate release from photoreceptors (Cadetti and Thoreson, 2006; Thoreson et al., 2008; Verweij et al., 1996). This process of "lateral inhibition" modulates signalling to postsynaptic bipolar cells and represents the first level of visual processing.

HCs are broadly categorized as axonless (A-type) or short-axon (B-type) cells. In teleost fish, axonless HCs connect exclusively with rods while short-axon HCs form subtype specific connections with cones (Song et al., 2008; Stell and Lightfoot, 1975). Goldfish have four HC

subtypes H1, H2, and H3 are short-axon cells that feedback onto different sets of cones, while H4 are specific to rods (Stell and Lightfoot, 1975). Subtypes H1-H4 are distinguished morphologically by the increasing size of their dendritic field, the decreasing size of their soma, increasing dendritic field to soma size ratio, and increasing distance from the photoreceptor layer (Country et al., 2021; Song et al., 2008; Stell and Lightfoot, 1975). Notably, in fish, only H1 subtypes are seen to accumulate and release the inhibitory neurotransmitter γ-aminobutyric acid (GABA) (Country et al., 2021; Marc et al., 1978; Paik et al., 2003). The subtype specific role for GABA in H1 cells and its potential implications on feedback are both unknown.

1.3.3 Lateral inhibition

Lateral inhibition is a HC mediated feedback loop that is involved in generating center-surround receptive fields necessary for edge detection, light-dark adaptation, and colour opponency. While it's known that HCs ultimately downregulate photoreceptors by inhibiting activation of presynaptic VGCCs (Cadetti and Thoreson, 2006; Verweij et al., 1996; Vessey et al., 2005), thus preventing Ca^{2+}-dependent glutamate release; the precise mechanism underlying the feedback between HCs and photoreceptors remains unclear.

Historically, three controversial hypotheses have described how feedback from HCs to photoreceptors might be mediated, including either the release of γ-aminobutyric acid (GABA), extracellular changes in pH, or via ephaptic coupling (Thoreson and Mangel, 2012). Recent work in mammals has put forward compelling evidence that HCs tonically release autaptically acting GABA to modulate synaptic cleft pH in a membrane voltage-dependant manner, influencing the activation of cone VGCCs and glutamate release (Grove et al. 2019). This

hybrid GABA-pH model puts forth that when HCs are depolarized by glutamate, the driving force of HCO_3^- efflux through GABA-gated Cl^- channel ($GABA_C$) autoreceptors is reduced while H^+ extrusion through the Na^+/H^+ exchanger increases to offset intracellular acidification (Barnes et al., 2020; Grove et al., 2019). This acidifies the cleft, inhibiting Ca^{2+} influx to photoreceptors through VGCC, and reduces glutamate release (Barnes et al., 2020; Grove et al., 2019). The opposite is described in the hyperpolarized HC where the increased driving force of HCO_3^- promotes alkalinization of the cleft and the subsequent activation of photoreceptor VGCCs, promoting glutamate release (Barnes et al., 2020; Grove et al., 2019). Whereas the GABA-pH pathway of feedback inhibition has gained support in mammalian retina, a similar mechanism in teleost retina has not yet been fully described. There is evidence of $GABA_C$ receptor activation in white perch retina (Qian and Dowling, 1993), although $GABA_C$ receptors were not successfully characterized in goldfish retina, perhaps owing to a lack of a reliable marker (Koulen et al., 1997).

1.3.4 Glutamate responses in horizontal cells

Glutamate is the major excitatory neurotransmitter of the CNS. There are two major categories of glutamate receptors: the iGluRs, such as those described in section 1.2.1, and metabotropic glutamate receptors (mGluRs), which are G-protein-coupled receptors. Although mGluRs are present in the teleost retina, these receptors influence cellular responses through second messengers and do not form ion channels (Beraudi et al., 2007; Linn and Gafka, 1999).

During glutamate stimulation, HCs exhibit a distinctive profile of changes in $[Ca^{2+}]_i$ over time. This response is characterized by an initial, large, transient peak in $[Ca^{2+}]_i$ upon glutamate

application, followed by a decrease in $[Ca^{2+}]_i$ to a sustained, elevated plateau that is maintained for as long as glutamate is present (Hayashida and Yagi, 2002). Glutamate binds to iGluRs and enables the non-specific passage of small cations; while this predominantly facilitates transport of Na^+ and K^+ across the plasma membrane, small amounts of Ca^{2+} also enter the cell through Ca^{2+}-permeable iGluRs. The peak phase of the $[Ca^{2+}]_i$ response to glutamate reflects the mass release of stored Ca^{2+} from the endoplasmic reticulum (ER) through CICR via ryanodine receptors in response to this subtle increase in $[Ca^{2+}]_i$ (Huang et al., 2004). The remainder of the glutamate response, the plateau phase, reflects Ca^{2+} entry through iGluRs and VGCCs which persists for as long as glutamate is present to depolarize the cell (Linn and Christensen, 1992; Tachibana, 1983). Given the constant influx of Ca^{2+} during periods of low light, HCs must employ efflux, sequestration, and buffering methods to repolarize the cell and maintain survivable $[Ca^{2+}]_i$ (Country and Jonz, 2017). This is an energetically costly process that depends upon sufficient ATP production to fuel the active transporters, such as plasma membrane Ca^{2+}-ATPases (PMCAs) and sarcoplasmic/endoplasmic reticulum Ca^{2+}-ATPases (SERCAs) (Hayashida et al., 1998).

1.4 Thesis objectives

Considering the tonic activation of glutamate receptors in HCs that occurs in the retina, the present thesis examines the effects of hypoxia on $Ca^{2+}{}_i$ dynamics of isolated hypoxia-tolerant goldfish HCs during glutamate responses. Using ratiometric Ca^{2+} imaging, we test the hypothesis that, under constant stimulation of HCs by glutamate, mK_{ATP} would continue to regulate $[Ca^{2+}]_i$ during hypoxia.

To study Ca^{2+} dynamics in live goldfish HCs, we used the Ca^{2+}-sensitive fluorescent dye, Fura-2, to measure changes in $[Ca^{2+}]_i$ during application of glutamate and hypoxia. This experimental approach was used to address the following research objectives:

- Identify if hypoxia increases $[Ca^{2+}]_i$ during glutamate responses in HCs compared to glutamate responses in normoxia.
- Assess whether regulation of $[Ca^{2+}]_i$ during hypoxia is dependent upon mK_{ATP} channels.
    - If $[Ca^{2+}]_i$ regulation is mK_{ATP} channel dependent, we predict that no hypoxia-dependant $[Ca^{2+}]_i$ increase will be observed during pharmacological inhibition of the mK_{ATP} channels.
- Identify the source (i.e. intracellular and/or extracellular) of the increased $[Ca^{2+}]_i$ observed during glutamate responses in hypoxia by selectively blocking Ca^{2+}-permeable pathways.
    - If extracellular Ca^{2+} is the source of the increase $[Ca^{2+}]_i$, we predict that no hypoxia-dependant $[Ca^{2+}]_i$ increase will be observed during glutamate application in Ca^{2+}-free solution.
    - If L-type voltage gated Ca^{2+} channels, ryanodine receptors, or the mitochondrial Ca^{2+} uniporter are responsible for the increase $[Ca^{2+}]_i$, we predict that no hypoxia-dependant $[Ca^{2+}]_i$ increase will be observed during pharmacological inhibition of these channels.

Not only does this work contribute to our growing understanding of $[Ca^{2+}]_i$ regulation in hypoxia-tolerant neurons, but it also provides insights to the potential role HCs play in vision and as a driver of larger-scale neuronal suppression during prolonged hypoxic insult. This thesis

concludes by proposing a strategy through which goldfish HCs may initiate a response to hypoxia in the retina that includes a neuroprotective reduction in the activity of the outer retina.

2. METHODS

2.1 Ethical approval

All procedures for animal care and handling were carried out under the approval of the University of Ottawa Animal Care and Veterinary Services (ACVS) protocol BL-3667, in accordance with regulations set out by the Canadian Council on Animal Care (CCAC). Adult common goldfish (*Carassius auratus*, Linnaeus 1758) were procured from Mirdo Importations Canada (Montreal, QC, Canada) and maintained at the University of Ottawa Laboratory for the Physiology and Genetics of Aquatic Organisms. Fish were maintained at 18°C in a constant flow-through system, where they were provided with fresh, aerated and dechloraminated water. Tank photoperiod was continuously cycled between 12 h light:12 h dark. Goldfish ranging between 7 g and 39 g were dark-adapted for approximately 1 h prior to being euthanized by concussion and decapitation. All datasets presented in this study are from recordings of cells from both male and female individuals.

2.2 Isolated cell preparation

HC isolation was performed in low-light and closely followed the methodology laid out by Jonz and Barnes (2007). Unless otherwise stated, all chemicals were sourced from Sigma-Aldrich (Oakville, ON, Canada). Eyes were removed and placed in cold Ca^{2+}-free Ringer's solution (Table 1). Eyes were hemisected posterior to the ora serrata and lenses were removed. Whole retinas were then separated from eyecups and placed in hyaluronidase (100 U ml^{-1}, cat. no. H-3506) in modified L-15 solution for 20 min at room temperature to degrade the vitreous humour. L-15 solution was comprised of 70% Leibovitz's medium and 30% Ca^{2+}-free Ringer's

solution. Retinas were washed for 3 min in fresh L-15 solution 3 times before being transferred to L-15 solution containing 7 U ml^{-1} papain (cat. no. 3126, Worthington Biochemical Corporation, Lakewood, NJ, USA), previously activated with 2.5 mM L-cysteine, for 45 min to enzymatically dissociate cells. Retinas were washed again 3 times for 3 min in L-15 solution. Small portions of retina (~2 mm^2) were cut and gently triturated 3 times using a Pasteur pipette. These sections of tissue were then placed in 3 ml of normal extracellular solution (ECS, Table 1), containing 5 μM of a membrane-permeant form of the Ca^{2+} indicator dye, Fura-2 (Fura-2-LeakRes-AM; Ion Biosciences, San Marcos, TX, USA, cat. no. 1061), and 0.1% of a 10% Pluronic F-127 solution (cat. no. P2443). In the dye solution, tissue was triturated 5-8 times to mechanically dissociate the cells. The resulting cell suspension was then transferred to 35 mm culture dishes (Corning Inc., Bedford, MA, USA) fitted with perfusion chambers (Warner Instruments Inc, Hamden, CT, USA, cat. no. RC-33DL). Prior to chamber assembly, culture dishes were pre-coated with 0.01% poly-L-lysine (cat. no. A-005-C) for 10 min, rinsed 3 times with double-distilled water, and allowed to dry completely. Cells were incubated in Fura-2 dye solution in darkness for 30 min. Each dish was then rinsed 3 times with dye-free ECS.

2.3 Relative $[Ca^{2+}]_i$ measurements

Ca^{2+} imaging protocols closely followed those outlined by Country et al. (2019). Prior to fluorescence imaging, HCs were identified by their characteristically large somata and thick dendrites (Dowling et al., 1985) using brightfield imaging with a compound microscope (FN-1, Nikon, Tokyo, Japan). Cells were recorded using a CCD camera (QImaging, Surrey, BC, Canada) and NIS Elements software (Nikon) by assigning circular regions of interest within HC somata to measure relative changes in fluorescence. Fluorescence imaging was accomplished

using a Lambda DG-5 wavelength changer (Sutter Instruments, Novato, CA, USA) programed to alternate between 340 and 380 nm excitation wavelengths once per second, and emission light was filtered through a 510 nm band pass filter in accordance with the ratiometric fluorescence properties of Fura-2 (Grynkiewicz et al., 1985). Light passed through a 40× water-immersion objective lens with a numerical aperture of 0.8 (MRF07420 CFI Fluor, Nikon) and optimized for UV transmission.

2.4 Experimental procedure and solutions

Using a gravity-driven system and peristaltic pump (Fisher Scientific, Ottawa, ON, Canada) cells were continuously superfused with ECS at ~1 ml min^{-1}. HCs typically remained viable for at least 4 h after isolation, as determined by the presence of spontaneous activity and their ability to maintain low baseline $[Ca^{2+}]_i$. In all experiments, cells were recorded for a minimum of 5 min in normoxic ECS before and after application of treatment solutions. HCs were exposed to 5 min of 100 µM glutamate (Country et al., 2019) three times: once in normoxia, once during the last 5 min of a 20-min exposure to hypoxia, and again during the last 5 min of a 10-min normoxic recovery period. Hypoxic solutions were produced by bubbling solution reservoirs with 100% N_2 for at least 30 min prior to superfusion, and throughout hypoxia treatments. This method results in a solution with a P_{O2} of ~25 mmHg. Normoxic (control) solutions were bubbled with compressed air at the same intensity and duration.

The role of mK_{ATP} channels in regulating $[Ca^{2+}]_i$ was tested using solutions containing 100 µM 5-hydroxydecanoic acid (5-HD), which blocks mK_{ATP} activity (Country and Jonz, 2021; Pamenter et al., 2008b). The potential involvement of extracellular Ca^{2+} sources on $[Ca^{2+}]_i$ was

tested by perfusing chambers with Ca^{2+}-free ECS, or by using solutions containing the L-type channel blocker, 100 μM verapamil (Schubert et al., 2006). Intracellular Ca^{2+} stores were similarly tested by co-applying glutamate with 20 μM ryanodine (Country et al., 2019; Huang et al., 2004), and the mitochondrial Ca^{2+} uniporter (MCU) was inhibited with 40 nM ruthenium red (Montero et al., 2001; Pamenter et al., 2008b). The chemical composition for all treatment solutions are summarized in Table 1.

2.5 Analysis

Fura-2 fluorescence ratios ($R_{340/380}$) were calculated by dividing the fluorescence emission intensity from 340 and 380 nm excitations. $R_{340/380}$ values are proportional to $[Ca^{2+}]_i$ and were generated by NIS Elements software before being exported to Excel (Microsoft Corp., Redmond, WA, USA) and Prism 8 (GraphPad Software Inc., San Diego, CA, USA) to identify the start and endpoints of the plateau phase for each response to glutamate. For each recording, a baseline was generated using Excel. This was performed by first determining the maximum and minimum range of $R_{340/380}$ during the first 5 min of recording and averaging all data points within the bottom 10% of that range to produce a single point. The same procedure was done for the final 5 min of the recording. A baseline was then calculated as the slope between those two points. Baseline values were subtracted from the initial $R_{340/380}$ to rule out the effects of changing baseline over time. The average $R_{340/380}$ of the plateau phase of each glutamate response was finally determined by calculating the mean baseline-subtracted $R_{340/380}$ between the start and endpoints assigned to each response.

Statistical analyses of all experiments were done in Prism 8. Data are presented as means ± SD. Comparison of glutamate responses were carried out using Friedman's test for repeated measures and Dunn's post-hoc test for multiple comparison. All column groups were tested with a level of significance of $P < 0.05$.

3. RESULTS

The data presented in this study are derived from recordings of 99 HCs isolated from 50 goldfish (26 male; 24 female). Relative changes in $[Ca^{2+}]_i$ were recorded during brief exposures to 100 μM glutamate using the ratiometric Ca^{2+}-imaging dye, Fura-2. Responses to glutamate were similar to those previously reported in HCs (Country et al., 2019). Cells responded immediately to the application of glutamate with a large, transient rise in $[Ca^{2+}]_i$, followed by a sustained, elevated $[Ca^{2+}]_i$ for as long as glutamate was applied. HCs returned to baseline $[Ca^{2+}]_i$ shortly after reperfusion with normal solution. Figure 2 depicts a representative goldfish HC and the time-course of ratiometric changes ($R_{340/380}$) related to $[Ca^{2+}]_i$ in response to glutamate. HCs also display spontaneous, Ca^{2+}-based action potentials when not exposed to glutamate (Country et al., 2019) and are visible in Figure 2 and subsequent figures.

3.1 Hypoxia further increased $[Ca^{2+}]_i$ when horizontal cells were exposed to glutamate

To test the hypothesis that hypoxia would change $[Ca^{2+}]_i$ during the glutamate response in goldfish HCs, we measured mean $R_{340/380}$ of the plateau phase in normoxia and hypoxia in the same cells. We first established a procedure in which HCs were exposed to three successive bouts of glutamate (Fig. 3A). Under conditions of normoxia, HCs displayed a uniform change in mean $[Ca^{2+}]_i$ during the first and second applications of glutamate (Fig. 3B, N=9 [5 males; 4 females]). There was, however, a slightly greater increase in $[Ca^{2+}]_i$ observed in 89% of cells during the third glutamate response that was significantly greater than the first response (Fig. 3B, P=0.0286). We made similar observations in other experiments (Fig. 4B, P=0.0230; Fig. 6D, P=0.0133). This increase was associated with the shorter recovery period between the second

and third application of glutamate (5 min), compared to the longer recovery period following the first application (15 min). The shorter recovery period was imposed to minimize the overall duration of recordings in our experiments and to preserve cell viability, and had no negative effects on our ability to deduce the effects of hypoxia in subsequent experiments.

Horizontal cells displayed a significantly greater rise in $[Ca^{2+}]_i$ during the plateau phase of glutamate application after cells had been exposed to hypoxia for 15 min, compared to responses to glutamate before and after co-administration of hypoxia (Fig. 3C,D, N=15 [6 males; 4 females], P=0.0016). Of the 15 cells tested in Figure 3D, 14 displayed a reversible increase in $[Ca2+]_i$ produced by hypoxia, whereas the other 1 cell responded to hypoxia but did not recover. The effects of hypoxia in the presence of glutamate corresponded to a 1.3-fold ± 0.05 increase in $[Ca2+]_i$ over glutamate alone.

3.2 Blocking mitochondrial K_{ATP} channels prevented the hypoxia-dependent rise in $[Ca^{2+}]_i$ during glutamate application

Goldfish HCs are dependent upon mK_{ATP} channels to stabilize $[Ca^{2+}]_i$ and protect the cell against hypoxic insult, and this mechanism is blocked by the mK_{ATP} channel inhibitor, 5-HD (Country and Jonz, 2021). We first measured mean $[Ca^{2+}]_i$ of glutamate responses before, during, and after application of 5-HD, to control for the potential effects of 5-HD on these cells (Fig. 4A). 5-HD alone had no effect on mean $[Ca^{2+}]_i$ of the glutamate response (Fig. 4B, N=18 [5 males; 1 female]). To test whether the mK_{ATP}-driven pathway was contributing to the increased $[Ca^{2+}]_i$ observed during the glutamate response in hypoxia, we performed hypoxia experiments in the presence of 5-HD (Fig. 4C). During mK_{ATP} inhibition by 5-HD, there was no difference between the hypoxic glutamate response and the preceding glutamate response in normoxia (Fig. 4D, N=18 [3 males; 5 females]). There was, however, a significant decrease in

$[Ca^{2+}]_i$ observed during the third application of glutamate relative to the first and second applications (Fig. 4D, both P=0.0081). This may have been caused by an additional suppressive effect on $[Ca^{2+}]_i$ due to the prolonged application of 5-HD in these experiments. Taken together, these results indicate that mK_{ATP} channel activity contributes to the rise in $[Ca^{2+}]_i$ during the hypoxic glutamate response.

3.3 Extracellular Ca^{2+} did not contribute to the increase in $[Ca^{2+}]_i$ during hypoxia

Goldfish HCs are known to express high threshold and sustained L-type VGCCs, which are tonically activated during prolonged depolarization induced by glutamate application (Hayashida et al., 1998; Tachibana, 1983). We tested whether the increased mean $[Ca^{2+}]_i$ during the hypoxic glutamate response was the result of Ca^{2+} influx through L-type channels. Application of the L-type channel inhibitor, 100 μM verapamil, on its own moderately suppressed the rise in $[Ca^{2+}]_i$ during the plateau phase of the glutamate response, consistent with previous reports of L-type channel inhibition in HCs (Hayashida et al., 1998). This can be observed in our experiments when comparing the response to the first bout of glutamate in the presence of verapamil (Fig. 5A) with the response to glutamate alone (Fig. 3A). Despite the mild, suppressive effect of verapamil on the glutamate response, the hypoxia-dependent increase in $[Ca^{2+}]_i$ persisted upon glutamate application (Fig. 5A). Mean $[Ca^{2+}]_i$ of the hypoxic glutamate response in the presence of verapamil was significantly greater than in normoxia (Fig. 5B, N=8 [2 males; 2 females], P=0.0179). This indicated that L-type VGCCs did not contribute significantly to the rise in $[Ca^{2+}]_i$ observed during the glutamate response in hypoxia.

We next tested whether the $[Ca^{2+}]_i$ increase observed during hypoxia may have arisen from an extracellular source more generally by applying glutamate in Ca^{2+}-free recording solution. For example, some glutamate receptors in teleost HCs are themselves permeable to Ca^{2+} and may allow for Ca^{2+} influx from the extracellular space during activation (Country and Jonz, 2017). In Ca^{2+}-free solution, HCs exhibited the typically large, transient increase in $[Ca^{2+}]_i$ upon glutamate application, but the plateau phase was suppressed in the absence of extracellular Ca^{2+} (Fig. 5C). This aligns with previous observations made in Ca^{2+}-free solution during the glutamate response (Country et al., 2019). Importantly, even in the absence of extracellular Ca^{2+}, in all cells tested hypoxia further increased $[Ca^{2+}]_i$ during the glutamate response (Fig. 5C, arrowhead). The increase in $[Ca^{2+}]_i$ was small but significant when compared to normoxic controls (Fig. 5D, N=12 [3 males; 3 females], P=0.0128). These results indicate that extracellular Ca^{2+} was not an important source for the hypoxia-dependent rise in $[Ca^{2+}]_i$.

3.4 The hypoxia-dependent rise in $[Ca^{2+}]_i$ was inhibited by blocking intracellular stores

The mitochondria and ER are important sites for regulating $[Ca^{2+}]_i$ in neurons, including HCs of teleost retina (Country and Jonz, 2017; Hille, 2001). Based on the established roles of mK_{ATP} channels in neuroprotection (Country and Jonz, 2021; Pamenter et al., 2008b), we examined whether the MCU may participate in regulating $[Ca^{2+}]_i$ in HCs during hypoxia. We blocked MCU by applying ruthenium red (40 nM) with glutamate (Fig. 6A). During this procedure, we observed no significant change in the $[Ca^{2+}]_i$ response to glutamate in hypoxia compared with glutamate in normoxia (Fig. 6B, N=14 [1 male; 3 females]).

Non-mitochondrial Ca^{2+} stores in teleost HCs are often associated with the involvement of s, which mediate Ca^{2+} release from the ER during the peak phase of the glutamate response (Country and Jonz, 2017; Huang et al., 2004; Linn and Gafka, 2001; Linn and Christensen, 1992) To test their potential involvement in the hypoxic glutamate response described in the present study, we inhibited ryanodine receptors by co-application of ryanodine (20 μM) with glutamate (Fig. 6C). Co-application of glutamate and ryanodine yielded no significant difference between the response to glutamate under hypoxia and normoxic control (Fig. 6D, N=5 [1 male; 2 females]), indicating that ryanodine receptor activity is required for the hypoxia-dependent rise in $[Ca^{2+}]_i$.

Figure 2. Fura-2 measurement of $[Ca^{2+}]_i$ during a characteristic glutamate response in isolated horizontal cells. (A-D) Pseudocolour representation of fluorescence images depicting relative changes in $[Ca^{2+}]_i$ during a glutamate response in an isolated goldfish HC. Colours were coded relative to the ratio of the intensity of fluorescence emission following excitation at 340 nm and 380 nm. High ratios (yellow/green) correspond to higher $[Ca^{2+}]_i$, whereas low ratios (indigo/violet) correspond to low $[Ca^{2+}]_i$, in accordance with the scale on the right. Peak response to glutamate is captured in B. (E) HCs were identified using brightfield microscopy prior to Fura-2 Ca^{2+} imaging. (F) A representative trace of the cell presented in A-E illustrating the fluorescence ratio ($R_{340/380}$), which is proportional to $[Ca^{2+}]_i$, over time. Dashed vertical lines indicate timepoints of the fluorescence images, which were taken before (a), at peak phase (b), plateau phase (c), and after (d) the response to 100 μM glutamate application. Also depicted in F is a spontaneous Ca^{2+} transient immediately preceding peak phase. Scale bars in D and E = 25 μm. Scales in F indicate the Fura-2 fluorescence ratio ($R_{340/380}$) and time in seconds (s).

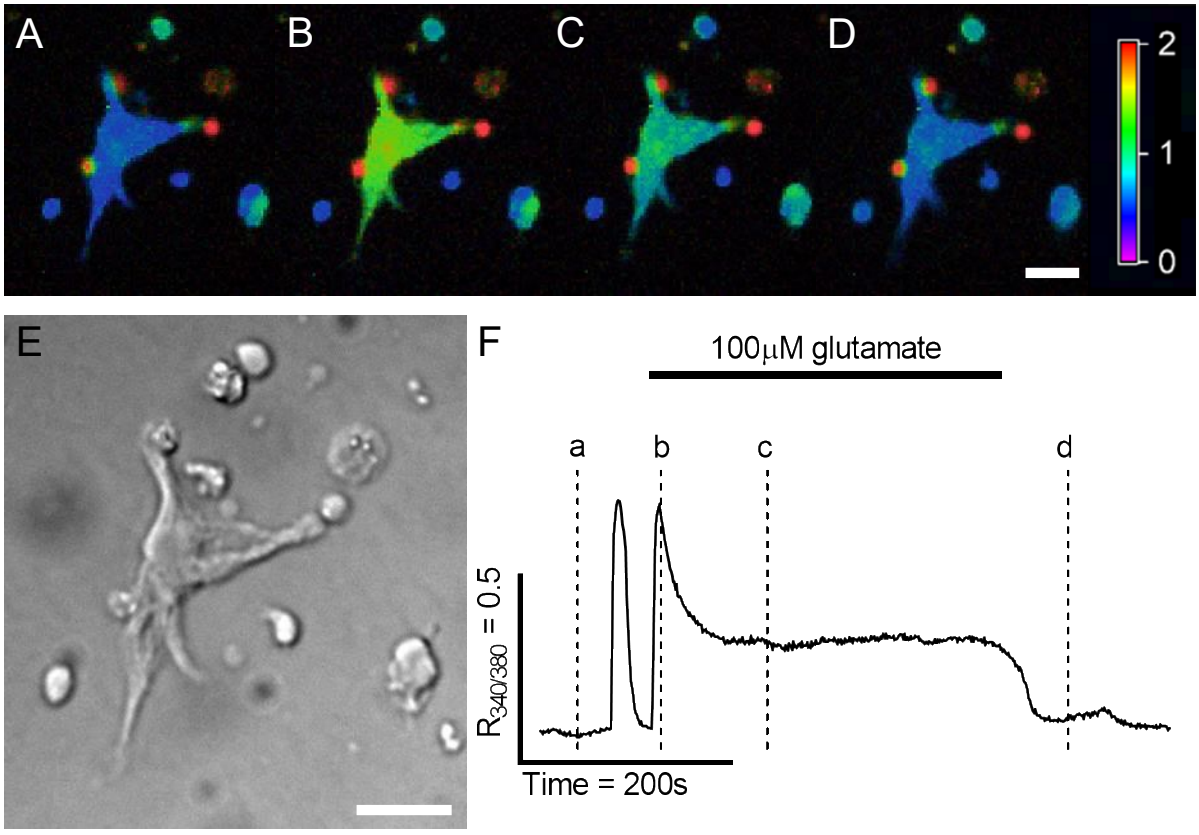

Figure 2

Figure 3. $[Ca^{2+}]_i$ during the plateau phase of the glutamate response was greater in hypoxia than in normoxia. (A) Representative recording of a goldfish HC exposed to three consecutive applications of 100 μM glutamate (bars) under normal (normoxic) conditions. (B) Summary data of mean ± SD $R_{340/380}$ of the plateau phase during glutamate responses corresponding to experiments in panel A (N=9). (C) When cells were subjected to hypoxia (long bar), $[Ca^{2+}]_i$ of the plateau phase of the glutamate response was greater than during normoxia. (D) Summary data of mean ± SD $R_{340/380}$ from glutamate responses in normoxia and hypoxia corresponding to experiments in panel C. Asterisk indicates a significant increase during hypoxia (N=15, P=0.0016, Friedman's and Dunn's tests). Scale bars in A and C indicate the Fura-2 fluorescence ratio ($R_{340/380}$) and time in seconds (s).

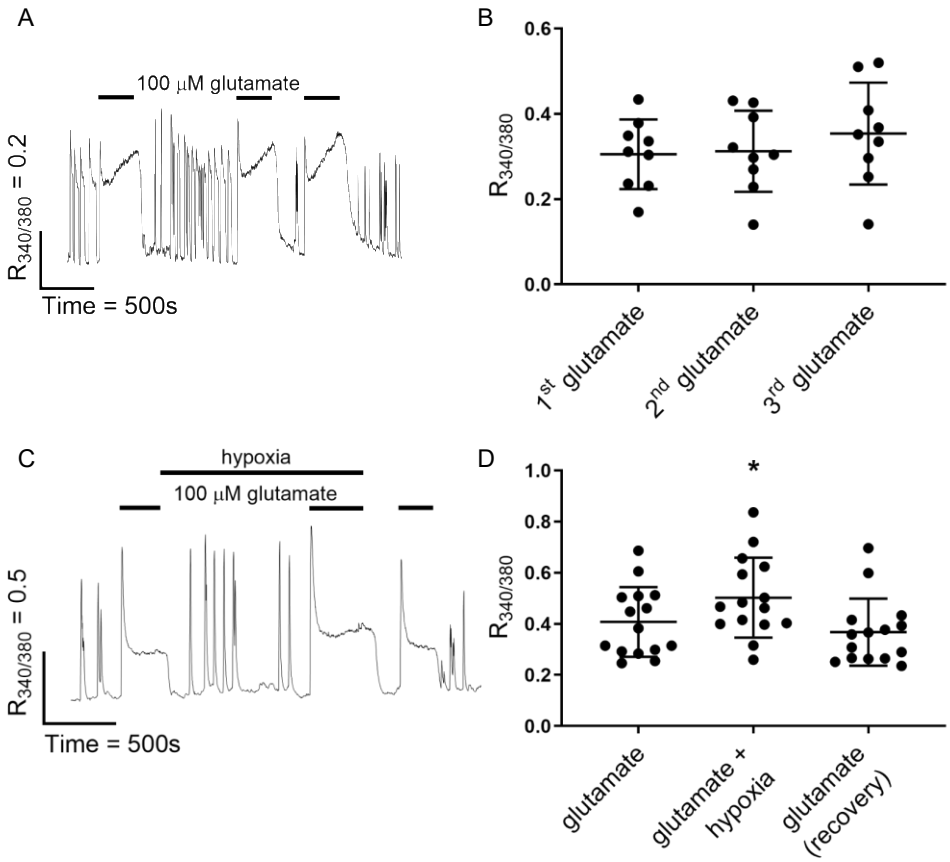
A
100 μM glutamate
R340/380 = 0.2
Time = 500s
B
R340/380
0.6
0.4
0.2
0.0
1st glutamate
2nd glutamate
3rd glutamate
C
hypoxia
100 μM glutamate
R340/380 = 0.5
Time = 500s
D
R340/380
1.0
0.8
0.6
0.4
0.2
0.0
*
glutamate
glutamate + hypoxia
glutamate (recovery)

Figure 3

Figure 4. Blockade of mK_{ATP} channels eliminated the effects of hypoxia upon $[Ca^{2+}]_i$ during the plateau phase of the glutamate response. (A) Representative recording of a goldfish HC exposed to 100 μM glutamate and 100 μM 5-hydroxydecanoic acid (5-HD, bars). (B) Summary data of mean ± SD $R_{340/380}$ glutamate responses demonstrated that the plateau phase was not affected by 5-HD alone (N=18). (C) When cells were subjected to hypoxia in the presence of 100 μM 5-HD, $[Ca^{2+}]_i$ of the plateau phase of the glutamate response did not change compared to the normoxic control. (D) Summary data of mean ± SD $R_{340/380}$ from glutamate responses under hypoxia demonstrated that 5-HD inhibited the hypoxia-dependent rise in $[Ca^{2+}]_i$ in the presence of glutamate (N=18, Friedman's and Dunn's tests). Scale bars in A and C indicate the Fura-2 fluorescence ratio ($R_{340/380}$) and time in seconds (s).

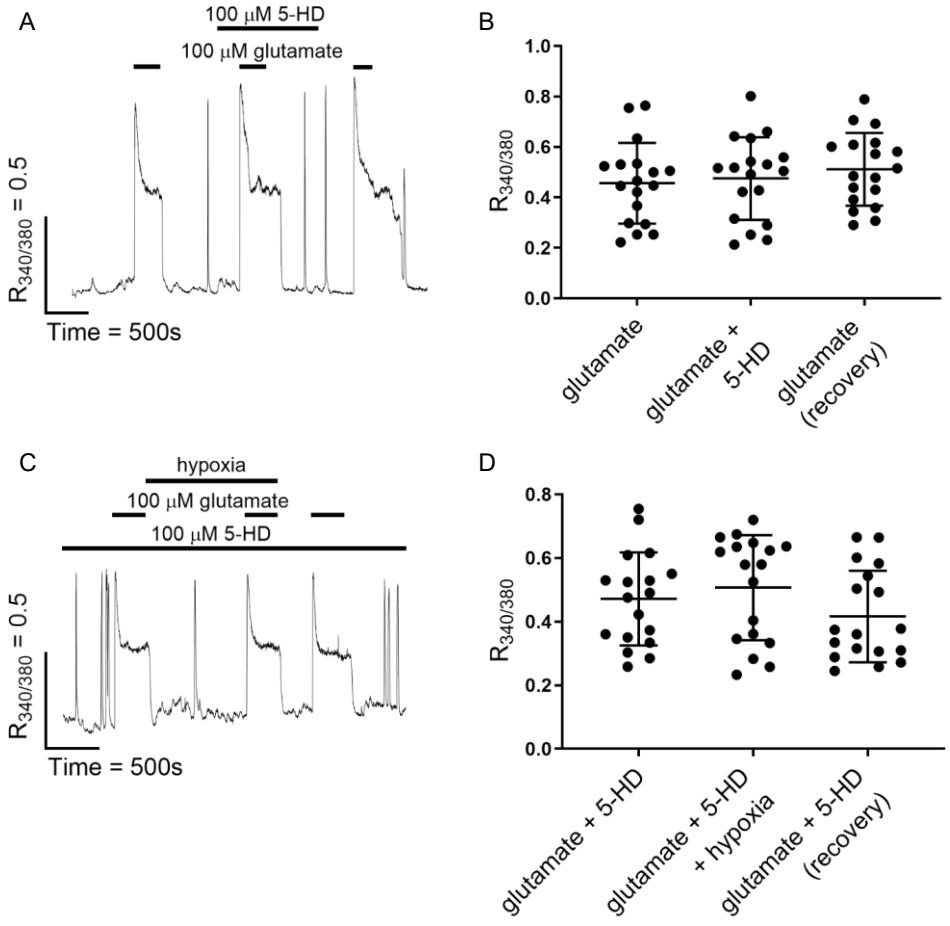
A
100 μM 5-HD
100 μM glutamate
R340/380 = 0.5
Time = 500s
B
R340/380
1.0
0.8
0.6
0.4
0.2
0.0
glutamate
glutamate + 5-HD
glutamate (recovery)
C
hypoxia
100 μM glutamate
100 μM 5-HD
R340/380 = 0.5
Time = 500s
D
R340/380
0.8
0.6
0.4
0.2
0.0
glutamate + 5-HD
glutamate + 5-HD + hypoxia
glutamate + 5-HD (recovery)

Figure 4

Figure 5. The rise in $[Ca^{2+}]_i$ during the plateau phase of the glutamate response during hypoxia was not eliminated by blocking L-type Ca^{2+} channels or removing extracellular Ca^{2+}. (A) Representative recording of $[Ca^{2+}]_i$ in a goldfish HC exposed to 100 μM glutamate during hypoxia showed increased $R_{340/380}$ despite application of 100 μM verapamil (bars). (B) Summary data of mean $R_{340/380}$ demonstrates inhibition of Ca^{2+} channels did not prevent the significant rise in $[Ca^{2+}]_i$ observed during hypoxia compared to normoxia (N=8, P=0.0179, Friedman's and Dunn's tests). (C) The elevated plateau phase in hypoxia (arrowhead) was observed in Ca^{2+}-free recording solution. The horizontal dashed baseline highlights the rise in $[Ca^{2+}]_i$ during hypoxia compared to normoxia. (D) Summary data of mean $R_{340/380}$ from hypoxic glutamate responses compared to normoxic control in the absence of extracellular Ca^{2+}. Asterisk indicates a significant increase in $[Ca^{2+}]_i$ during hypoxia compared to the first application of glutamate (N=12, P=0.0128, Friedman's and Dunn's tests). Scale bars in A and C indicate the Fura-2 fluorescence ratio ($R_{340/380}$) and time in seconds (s).

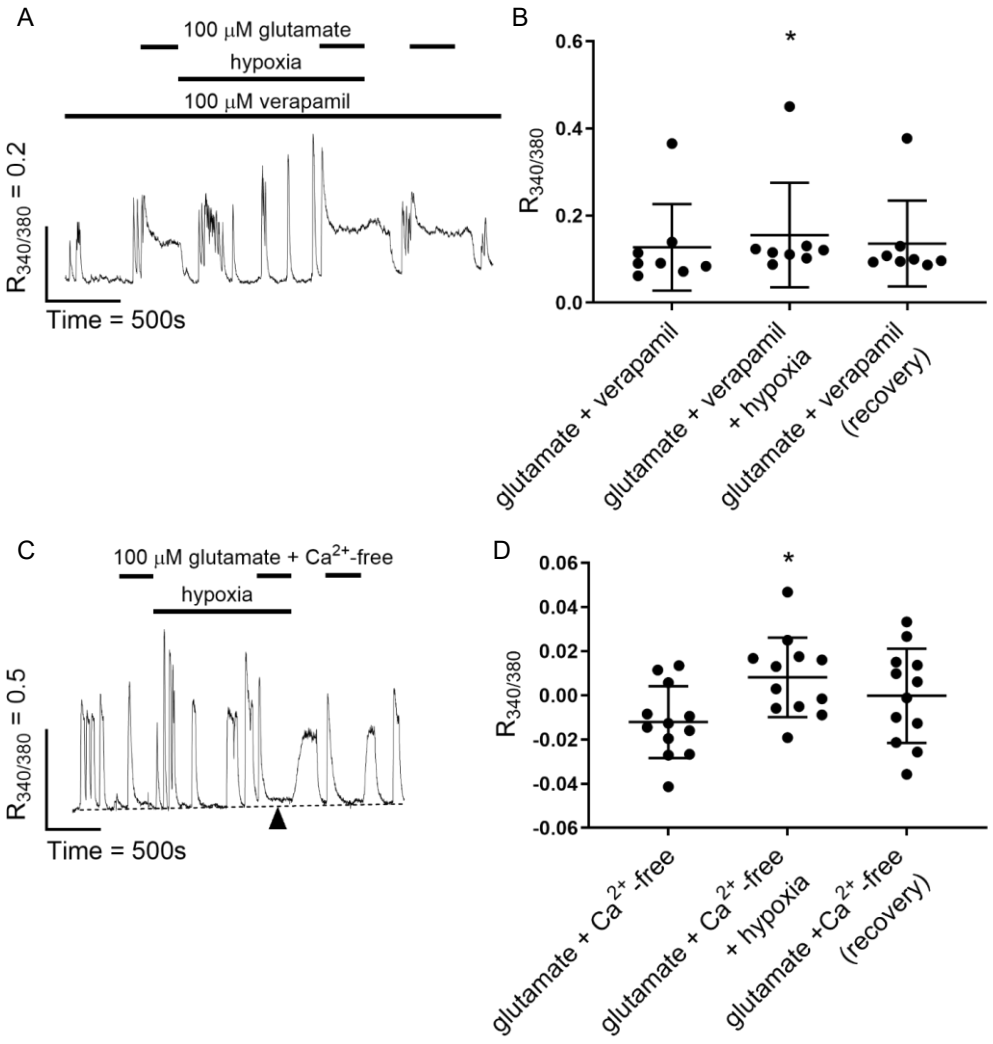
A
100 μM glutamate
hypoxia
100 μM verapamil
R340/380 = 0.2
Time = 500s
B
R340/380
0.6
0.4
0.2
0.0
*
glutamate + verapamil
glutamate + verapamil + hypoxia
glutamate + verapamil (recovery)
C
100 μM glutamate + Ca2+-free
hypoxia
R340/380 = 0.5
Time = 500s
D
R340/380
0.06
0.04
0.02
0.00
-0.02
-0.04
-0.06
*
glutamate + Ca2+ -free
glutamate + Ca2+ -free + hypoxia
glutamate +Ca2+ -free (recovery)

Figure 5

Figure 6. The effects of hypoxia upon the plateau phase of the glutamate response was abolished when the mitochondrial Ca^{2+} uniporter (MCU) or ryanodine receptors were inhibited. (A) Co-application of 100 μM glutamate and 40 nM ruthenium red inhibited the hypoxia-dependent rise in $[Ca^{2+}]_i$ during the plateau phase. (B) Summary data of mean $R_{340/380}$ from hypoxic glutamate responses compared to normoxic control were not impacted by hypoxia when MCU was inhibited using ruthenium red (N=14, Friedman's and Dunn's tests). (C) Representative recording of a goldfish HC following co-application of 100 μM glutamate and 20 μM ryanodine (bars). $[Ca^{2+}]_i$ during the plateau phase between normoxia and hypoxia was unchanged. (D) Summary data of mean $R_{340/380}$ of the plateau phase demonstrate that the rise in $[Ca^{2+}]_i$ caused by hypoxia was prevented by inhibition of ryanodine receptors (N=5, Friedman's and Dunn's tests). Scale bars in A and C indicate the Fura-2 fluorescence ratio ($R_{340/380}$) and time in seconds (s).

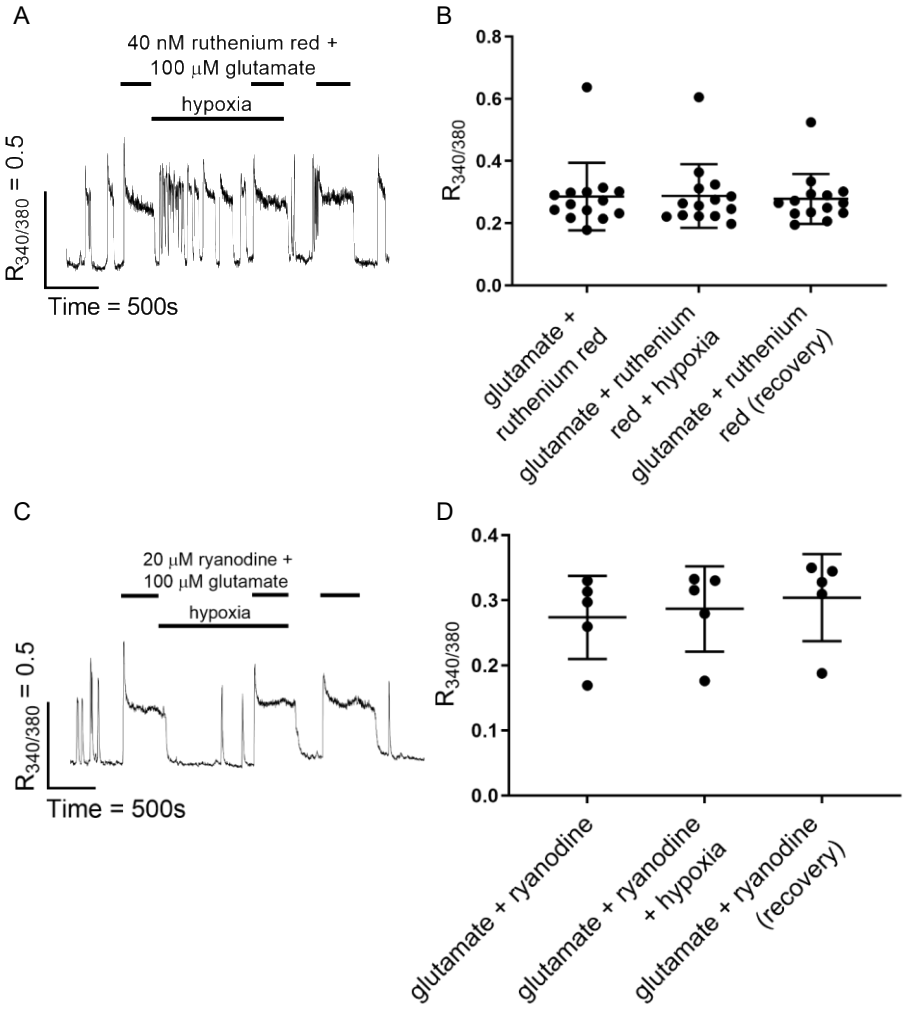
A
40 nM ruthenium red +
100 μM glutamate
hypoxia
R340/380 = 0.5
Time = 500s
B
R340/380
0.8
0.6
0.4
0.2
0.0
glutamate + ruthenium red
glutamate + ruthenium red + hypoxia
glutamate + ruthenium red (recovery)
C
20 μM ryanodine +
100 μM glutamate
hypoxia
R340/380 = 0.5
Time = 500s
D
R340/380
0.4
0.3
0.2
0.1
0.0
glutamate + ryanodine
glutamate + ryanodine + hypoxia
glutamate + ryanodine (recovery)

Figure 6

Table 1. Composition of Ringer's and extracellular solutions (ECS).

For all solutions, pH was adjusted to 7.80 (± 0.01) with NaOH.

		Extracellular solutions (ECS, in mM)								
Reagent	Ca^{2+}-free Ringer's	Normal ECS	Glutamate	Ca^{2+}-free + glutamate	Verapamil	Verapamil + glutamate	Ryanodine + glutamate	Ruthenium red + glutamate	5-HD	5-HD + glutamate
NaCl	120	120	120	120	120	120	120	120	120	120
KCl	2.6	5	5	5	5	5	5	5	5	5
$CaCl_2$	-	2.5	2.5	-	2.5	2.5	2.5	2.5	2.5	2.5
$MgCl_2$	-	2	2	4.5	2	2	2	2	2	2
Glucose	10	10	10	10	10	10	10	10	10	10
HEPES	10	10	10	10	10	10	10	10	10	10
NaH_2PO_4	0.5	-	-	-	-	-	-	-	-	-
Glutamate	-	-	0.1	0.1	-	0.1	0.1	0.1	-	0.1
Verapamil	-	-	-	-	0.1	0.1	-	-	-	-
Ryanodine[1]	-	-	-	-	-	-	0.02	-	-	-
Ruthenium red	-	-	-	-	-	-	-	0.00004	-	-
5-HD[1,2]	-	-	-	-	-	-	-	-	0.1	0.1

[1]Indicates compounds first dissolved in dimethyl sulfoxide (DMSO), which never surpassed a final concentration of 0.25% v/v.
[2]5-hydroxydecanoic acid.

4. DISCUSSION

The present study demonstrates that HCs isolated from the retina of hypoxia-tolerant goldfish maintain greater $[Ca^{2+}]_i$ during glutamate stimulation in hypoxia than in normoxia. Extracellular Ca^{2+} sources did not significantly contribute to this difference. Instead, we attribute the increase in $[Ca^{2+}]_i$ to activation of mK_{ATP} channels during hypoxia and intracellular pathways involving the mitochondria and ER. In light of a previous report that $[Ca^{2+}]_i$ was not increased by hypoxia in unstimulated HCs (Country and Jonz, 2021), our data suggest that goldfish HCs do not rely on a single strategy for protection against hypoxia in the retina.

4.1 Hypoxia tolerance in the CNS and retina

Overexcitation of glutamate receptors is a major component of excitotoxicity in neurons (Choi et al., 1987). The subsequent influx of Na^+ and Ca^{2+} activates energetic signalling pathways and rapidly depletes ATP (Choi, 1985; Else, 1991). In the retina, darkness stimulates photoreceptors to continuously release glutamate onto postsynaptic neurons, such as HCs, which then undergo prolonged membrane depolarization (Tornqvist et al., 1988). It is therefore not surprising that the retina has some of the highest energy demands of any tissue in the CNS (Wong-Riley, 2010). The retina is highly susceptible to cell death during hypoxia, anoxia, and ischemia. In the hypoxia-intolerant mammalian retina, high extracellular glutamate levels are commonly observed alongside the induction of excitotoxic degeneration of neurons, likely promoting overstimulation of ionotropic glutamate receptors (Lucas and Newhouse, 1957; Neal et al., 1994).

Hypoxia tolerance in the retina has been most strongly demonstrated in *Carassius* spp. Electroretinograms of crucian carp showed a 90% reduction in responsiveness to transient light stimuli in dark-adapted retina within 1 h of anoxic perfusion, and full recovery of light responses upon normoxic reperfusion (Johansson et al., 1997). These results indicate that crucian carp temporarily supresses retinal activity during anoxia without any permanent loss of visual function. Studies on the congeneric goldfish also revealed hypoxia tolerance throughout the retina. Activation of group 2/3 mGluRs contributed to cell survival in slice preparations following 3 h of hypoxia and normoxic reperfusion (Beraudi et al., 2007). Furthermore, isolated goldfish HCs maintained baseline $[Ca^{2+}]_i$ in the absence of glutamate receptor activation throughout 1 h of hypoxia, compared to HCs from the hypoxia-intolerant rainbow trout, which underwent an irreversible increase in $[Ca^{2+}]_i$ within only 20 min of the same treatment (Country and Jonz, 2021).

4.2 A potential role for mK_{ATP} channel activation in HCs exposed to glutamate

The present study reports a subtle but significant hypoxia-induced *increase* in $[Ca^{2+}]_i$ during glutamate stimulation. Under conditions of glutamate receptor activation, HCs are relatively depolarized (Ishida et al., 1984), as would be expected in the retina under low-light or dark conditions when photoreceptors release large amounts of glutamate into the synaptic cleft. The additional increase in $[Ca^{2+}]_i$ between hypoxic and normoxic glutamate responses was dependent on mK_{ATP} channel activity, since the effect was abolished by 5-HD. Such a mechanism, where mK_{ATP} activation mediates increased $[Ca^{2+}]_i$, is reminiscent of a neuroprotective pathway in central neurons of the anoxia-tolerant turtle brain. During anoxia, when ATP concentration is low (Buck et al., 1998), mK_{ATP} channels in turtle neurons open and

depolarize the mitochondrial membrane. This leads to reduced uptake of Ca^{2+} by the MCU, or Ca^{2+} release by the mitochondrial permeability transition pore, thereby increasing $[Ca^{2+}]_i$ (Hawrysh and Buck, 2013; Pamenter et al., 2008b). Unique to the turtle brain, this "paradoxical" increase in $[Ca^{2+}]_i$ downregulates activation of glutamate receptors in the plasma membrane, thereby limiting subsequent Ca^{2+} influx and providing protection against excitotoxicity (Hawrysh and Buck, 2013; Pamenter et al., 2008b; Zivkovic and Buck, 2010). In the current study, we found that inhibiting the MCU with ruthenium red to block Ca^{2+} uptake by the mitochondria resulted in a predictable rise in $[Ca^{2+}]_i$ when co-applied with glutamate; but when hypoxia was co-applied with ruthenium red, no further rise in $[Ca^{2+}]_i$ was recorded. These data suggest a similar role for the MCU in mediating a paradoxical increase in $[Ca^{2+}]_i$ in hypoxia-tolerant goldfish HCs. Unlike the case in turtle brain, our observations that glutamate receptor activation is required for the hypoxia-induced increase in $[Ca^{2+}]_i$ in HCs would suggest that glutamate receptor activity was not downregulated, though future investigations designed to study receptor activity directly are required for clarification.

Intracellular Ca^{2+} stored within the ER is released by ryanodine receptors once $[Ca^{2+}]_i$ is elevated. This process is known as CICR and is an important functional element in HCs (reviewed by Country and Jonz, 2017). During the $[Ca^{2+}]_i$ response to glutamate, the initial transient rise in $[Ca^{2+}]_i$ is due to CICR and can be inhibited by ryanodine (Huang et al., 2004), and the CICR triggered by activation of glutamate receptors results in inhibition of VGCCs (Linn and Gafka, 2001). Spontaneous Ca^{2+} oscillations in isolated HCs are also mediated, in part, by ryanodine receptors (Country et al., 2019). Given the link between glutamate receptor activation and CICR, we investigated whether ryanodine receptors may have contributed to the hypoxia-induced elevation in $[Ca^{2+}]_i$. As predicted, inhibition of Ca^{2+} release from the ER by ryanodine

abolished the hypoxia-induced rise in $[Ca^{2+}]_i$ in the presence of glutamate. In light of our results that extracellular Ca^{2+} did not contribute to the hypoxic increase in $[Ca^{2+}]_i$, these data therefore implicate intracellular stores as an important source of Ca^{2+}. In this model, we propose that mK_{ATP} acts as a sensor of hypoxia and depolarizes the mitochondrial membrane, thereby limiting Ca^{2+} uptake into the mitochondria and slightly elevating cytosolic Ca^{2+} concentration. Mitochondrial membrane depolarization during hypoxia has been demonstrated in goldfish HCs and is dependent on activation of mK_{ATP} (Country and Jonz, 2021). In the presence of glutamate, when glutamate receptors are activated and CICR is already taking place, this would result in additional release of Ca^{2+} from the ER via ryanodine receptors.

4.3 Implications for hypoxia tolerance in the retina

The results of the present study, and those of Country and Jonz (2021), demonstrate that mK_{ATP} activity plays a key role in controlling $[Ca^{2+}]_i$ in goldfish HCs during hypoxia. When HCs are not stimulated by glutamate and in a relatively hyperpolarized state, hypoxic activation of mK_{ATP} is required to preserve $[Ca^{2+}]_i$ homeostasis (Country and Jonz, 2021); however, a direct link between mK_{ATP} and $[Ca^{2+}]_i$ was not identified in that study. By contrast, the present data suggest that HCs employ a different strategy for protection against hypoxia during glutamate receptor activation, when the plasma membrane is relatively depolarized and $[Ca^{2+}]_i$ is already elevated. But what would be the purpose of further increasing $[Ca^{2+}]_i$ during hypoxia? We propose that the additional rise in $[Ca^{2+}]_i$ that occurs during hypoxia, while paradoxical for protection of intracellular Ca^{2+} homeostasis, may ultimately have protective effects on other neurons in the retina.

Johansson et al. (1997) first proposed, in the anoxic crucian carp, that the inhibitory neurotransmitter, GABA, is released by interneurons of the retina, such as HCs or amacrine cells, and causes the temporary reduction in retinal activity during oxygen deprivation. In goldfish HCs, GABA is limited to the H1 subtype (Ayoub and Lam, 1987; Country et al., 2021; Lam and Steinman, 1971; Marc et al., 1978; Paik et al., 2003), the most abundant subtype of HCs in fish (Ariel et al., 1984; Country et al., 2021; Young and Dowling, 1984). In addition, HCs that are depolarized in darkness tonically release GABA (Marc et al., 1978; Yazulla, 1985). In mammalian retina, GABA is an important component of inhibitory feedback responses from HCs to cone photoreceptors (Barnes et al., 2020). Whereas HCs are involved in feedback in goldfish, feedback does not appear to be dependent upon GABA in fish (Verweij et al., 1996). Instead, in goldfish and zebrafish there is evidence that GABA may act broadly as a slow modulator of feedback or light/dark adaptation (Endeman et al., 2012; Klaassen et al., 2011; Klooster et al., 2004).

GABA is released from HCs in goldfish by Na^+-dependent transport, such as during membrane depolarization, and by Ca^{2+}-dependent vesicular release (Ayoub and Lam, 1985, 1987, 1984; Klooster et al., 2004; Schwartz, 2002). In addition, GABA receptors (e.g. $GABA_A$ and $GABA_C$) are present in neurons of the outer retina, such as HCs, photoreceptors or bipolar cells (Endeman et al., 2012; Klooster et al., 2004; Paik et al., 2003). Interestingly, because the equilibrium potential of Cl^- in HCs is more positive than the resting membrane potential, activation of GABA receptors may be excitatory in HCs but inhibitory on other retinal neurons (Djamgoz and Laming, 1987; Klooster et al., 2004; Miller and Dacheux, 1983). Results of the present study lead us to propose that, in the presence of glutamate, hypoxia may further elevate $[Ca^{2+}]_i$ to a level that may increase the Ca^{2+}-dependent portion of GABA release from HCs. In

the intact hypoxic retina, an increase in GABA release would feed back positively onto HCs to release more GABA, and have inhibitory (i.e. hyperpolarizing) effects on other cell types, such as photoreceptors or bipolar cells, thereby reducing their activity.

An increase in the release of GABA in the CNS may be a common strategy for anoxia-tolerant animals to survive prolonged periods of oxygen deprivation. Anoxia produces a five-fold increase in GABA release in the brain of crucian carp (Nilsson, 1992, 1990), whereas in the turtle brain anoxia causes an increase in extracellular GABA to 90-times the normal concentration (Nilsson and Lutz, 1991). (Hawrysh and Buck, 2019) more recently demonstrated that interneurons in turtle cortex increase their activity and GABA release during anoxia. Activation of GABA receptors in the anoxic turtle brain is an important strategy for supressing electrical activity in central neurons and avoiding excessive release of glutamate (Pamenter et al., 2011). A similar strategy of increased GABA release by HCs may be present in the retina of anoxia-tolerant fish, such as goldfish and crucian carp. GABA-induced hyperpolarization of neurons in the outer retina may account for the suppression of light-evoked responses in crucian carp during anoxia (Johansson et al., 1997), and may be important for limiting the release of glutamate to the extracellular space and reducing consumption of ATP required to maintain ionic gradients (Bickler and Buck, 1998; Lutz and Nilsson, 2004). Whether GABA release from HCs is increased during hypoxia, however, remains to be determined.

An additional effect of the elevation of $[Ca^{2+}]_i$ during hypoxia is that excessive influx of Ca^{2+} through VGCCs of the plasma membrane would be reduced, thereby preventing further excitotoxic influx of Ca^{2+} and potentially setting a limit on Ca^{2+}-dependent GABA release. In HCs from goldfish and channel catfish (*Ictalurus punctatus*), accumulation of intracellular Ca^{2+} led to inactivation of membrane Ca^{2+} channels (Linn and Gafka, 2001; Tachibana, 1983).

5. CONCLUSION

The present study demonstrates an increase in $[Ca^{2+}]_i$ in HCs during hypoxia that was dependent on mK_{ATP} channel activity. Unlike the mK_{ATP}-dependent stabilization of baseline $[Ca^{2+}]_i$ that occurred in unstimulated HCs (Country and Jonz, 2021), under conditions of continuous activation by glutamate, the resulting $[Ca^{2+}]_i$ response was further elevated by exposure to hypoxia. Future investigations may uncover the specific role of elevated $[Ca^{2+}]_i$ in goldfish HCs during hypoxia, and whether this may represent part of an integrated pathway to suppress broad retinal activity during prolonged oxygen deprivation.

REFERENCES

Ames, A., 1992. Energy requirements of CNS cells as related to their function and to their vulnerability to ischemia: A commentary based on studies on retina. Can. J. Physiol. Pharmacol. 70, S158-S164.

Ariel, M., Lasater, E.M., Mangel, S.C., Dowling, J.E., 1984. On the sensitivity of H1 horizontal cells of the carp retina to glutamate, aspartate and their agonists. Brain Res. 295, 179-183.

Ayoub, G.S., Lam, D.M., 1984. The release of γ-aminobutyric acid from horizontal cells of the goldfish (*Carassius auratus*) retina. J. Physiol. 355, 191-214.

Ayoub, G.S., Lam, D.M., 1985. The content and release of endogenous GABA in isolated horizontal cells of the goldfish retina. Vision Res. 25, 1187–1193.

Ayoub, G.S., Lam, D.M.., 1987. Accumulation of γ-aminobutyric acid by horizontal cells isolated from the goldfish retina. Vision Res. 27, 2027–2034.

Barnes, S., Grove, J.C.R., McHugh, C.F., Hirano, A.A., Brecha, N.C., 2020. Horizontal cell feedback to cone photoreceptors in mammalian retina: Novel insights from the GABA-pH hybrid model. Front. Cell Neurosci. 14:595064.

Baylor, D.A., Fuortes, M.G.F., O'Bryan, P.M., 1971. Receptive fields of cones in the retina of the turtle. J. Physiol. 214, 265–294.

Beraudi, A., Bruno, V., Battaglia, G., Biagioni, F., Rampello, L., Nicoletti, F., Poli, A., 2007. Pharmacological activation of mGlu2/3 metabotropic glutamate receptors protects retinal neurons against anoxic damage in the goldfish *Carassius auratus*. Exp. Eye Res. 84, 544–552.

Bickler, P.E., Buck, L.T., 1998. Adaptations of vertebrate neurons to hypoxia and anoxia: Maintaining critical Ca^{2+} concentrations. J. Exp. Biol. 201, 1141–1152.

Buck, L.T., Espanol, M., Litt, L., Bickler, P.E., 1998. Reversible decreases in ATP and PCr concentrations in anoxic turtle brain. Comp Biochem. Physiol. A Mol. Integr. Physiol. 120, 633–639.

Buck, L.T., Bickler, P.E., 1998. Adenosine and anoxia reduce N-methyl-D-aspartate receptor open probability in turtle cerebrocortex. J. Exp. Biol. 201, 289–297.

Cadetti, L., Thoreson, W.B., 2006. Feedback effects of horizontal cell membrane potential on cone calcium currents studied with simultaneous recordings. J Neurophysiol. 95, 1992–1995.

Chan, P.H., Fishman, R.A., Longar, S., Chen, S., Yu, A., 1985. Cellular and molecular effects of polyunsaturated fatty acids in brain ischemia and injury. Prog. Brain Res. 63, 227–235.

Choi, D.W., 1985. Glutamate neurotoxicity in cortical cell culture is calcium dependent. Neurosci. Lett. 58, 293–297.

Choi, D.W., 1990. Methods for antagonizing glutamate neurotoxicity. Cerebrovasc. Brain Metab. Rev. 2, 105–47.

Choi, D.W., Koh, J., Peters, S., 1988. Pharmacology of glutamate neurotoxicity in cortical cell culture: Attenuation by NMDA antagonists. J. Neurosci. 8, 185–196.

Choi, D.W., Maulucci-Gedde, M., Kriegstein, A., 1987. Glutamate neurotoxicity in cortical cell culture. J. Neurosci. 7, 357–368.

Country, M.W., Campbell, B.F.N., Jonz, M.G., 2019. Spontaneous action potentials in retinal horizontal cells of goldfish (*Carassius auratus*) are dependent upon L-type Ca^{2+} channels and ryanodine receptors. J. Neurophysiol. 122, 2284-2293.

Country, M.W., Htite, E.D., Samson, I.A., Jonz, M.G., 2021. Retinal horizontal cells of goldfish (*Carassius auratus*) display subtype-specific differences in spontaneous action potentials in situ. J. Comp. Neurol. 529, 1756–1767.

Country, M.W., Jonz, M.G., 2017. Calcium dynamics and regulation in horizontal cells of the vertebrate retina: lessons from teleosts. J. Neurophysiol. 117, 523–536.

Country, M.W., Jonz, M.G., 2021. Mitochondrial K_{ATP} channels stabilize intracellular Ca^{2+} during hypoxia in retinal horizontal cells of goldfish (*Carassius auratus*). J. Exp. Biol. 224.(18):jeb.242634

Djamgoz, M.B.A., Laming, P.J., 1987. Micro-electrode measurements and functional aspects of chloride activity in cyprinid fish retina: Extracellular activity and intracellular activities of L- and C-type horizontal cells. Vis. Res. 27, 1481–1489.

Dowling, J.E., 1987. The Retina: An Approachable Part of the Brain. Harvard University Press, Cambridge.

Dowling, J.E., Pak, M.W., Lasater, E.M., 1985. White perch horizontal cells in culture: methods, morphology and process growth. Brain Res. 360, 331–338.

Dowling, J.E., Ripps, H., 1973. Effect of magnesium on horizontal cell activity in the skate retina. Nature 242, 101–103.

Dykens, J.A., Stern, A., Trenkner, E., 1987. Mechanism of kainate toxicity to cerebellar neurons in vitro is analogous to reperfusion tissue injury. J Neurochem. 49, 1222–1228.

Else, P.L., 1991. Oxygen consumption and sodium pump thermogenesis in a developing mammal. Am. J. Physiol. 261, 1575–1578.

Endeman, D., Fahrenfort, I., Sjoerdsma, T., Steijaert, M., Ten Eikelder, H., Kamermans, M., 2012. Chloride currents in cones modify feedback from horizontal cells to cones in goldfish retina. J. Physiol. 590, 5581–5595.

Erecińska, M., Silver, I.A., 1994. Ions and energy in mammalian brain. Prog. Neurobiol. 43, 37-71.

Fernandes, J.A., Lutz, P.L., Tannenbaum, A., Todorov, A.T., Liebovitch, L., Vertes, R., 1997. Electroencephalogram activity in the anoxic turtle brain. Am. J. Physiol. 273, 911-919.

Frandsen, A., Schousboe, A., 1991. Dantrolene prevents glutamate cytotoxicity and Ca^{2+} release from intracellular stores in cultured cerebral cortical neurons. J. Neurochem. 56, 1075–1078.

Garlid, K.D., Paucek, P., 2003. Mitochondrial potassium transport: the K^+ cycle. Biochim. Biophys. Acta - Bioenerg. 1606, 23–41.

Grove, J.C.R., Hirano, A.A., de Los Santos, J., McHugh, C.F., Purohit, S., Field, G.D., Brecha, N.C., Barnes, S., 2019. Novel hybrid action of GABA mediates inhibitory feedback in the mammalian retina. PLoS Biol. 17:3000200.

Grynkiewicz, G., Poenie, M., Tsien, R.Y., 1985. A new generation of Ca^{2+} indicators with greatly improved fluorescence properties. J. Biol. Chem. 260, 3440–3450.

Hanley, P.J., Daut, J., 2005. K_{ATP} channels and preconditioning: A re-examination of the role of mitochondrial K_{ATP} channels and an overview of alternative mechanisms. J. Mol. Cell. Cardiol. 39: 17-50, 2005.

Hawrysh, P.J., Buck, L.T., 2013. Anoxia-mediated calcium release through the mitochondrial permeability transition pore silences NMDA receptor currents in turtle neurons. J. Exp. Biol. 216, 4375–4387.

Hawrysh, P.J., Buck, L.T., 2019. Oxygen-sensitive interneurons exhibit increased activity and GABA release during ROS scavenging in the cerebral cortex of the western painted turtle. J. Neurophysiol. 122, 466–479.

Hayashida, Y., Yagi, T., 2002. On the interaction between voltage-gated conductances and Ca^{2+} regulation mechanisms in retinal horizontal cells. J. Neurophysiol. 87, 172-182.

Hayashida, Y., Yagi, T., Yasui, S., 1998. Ca^{2+} regulation by the Na^+-Ca^{2+} exchanger in retinal horizontal cells depolarized by L-glutamate. Neurosci. Res. 31, 189–199.

Heidelberger, R., Thoreson, W.B., Witkovsky, P., 2005. Synaptic transmission at retinal ribbon synapses. Prog. Retin. Eye Res. 24, 682–720.

Herbert, C. V., Jackson, D.C., 1985. Temperature effects on the responses to prolonged submergence in the turtle *Chrysemys picta bellii*. II. metabolic rate, blood acid-base and ionic changes, and cardiovascular function in aerated and anoxic water. Physiol. Zool. 58, 670–681.

Hicks, J.M.T., Farrell, A.P., 2000. The cardiovascular responses of the red-eared slider (*Trachemys scripta*) acclimated to either 22 or 5°C: II. Effects of anoxia on adrenergic and cholinergic control. J. Exp. Biol. 203, 3775–3784.

Hille, B., 2001. Ion channels of excitable membranes, 3rd ed. ed. Sinauer associates, Sunderland.

Hochachka, P.W., 1986. Defense strategies against hypoxia and hypothermia. Science. 231, 234–241.

Holopainen, I.J., Pitkänen, A.K., 1985. Population size and structure of crucian carp (*Carassius carassius* (*L.*)) in two small, natural ponds in Eastern Finland. Ann. Zool. Fennici. 22, 397–406.

Huang, S.-Y., Lui, Y., Liang, P.-J., 2004. Role of Ca^{2+} store in AMPA-triggered Ca^{2+} dynamics in retinal horizontal cells. Neuroreport. 15, 2311–2315.

Hyvärinen, H., Holopainen, I.J., Piironen, J., 1985. Anaerobic wintering of crucian carp (*Carassius carassius L.*)--II. Annual dynamics of glycogen reserves in nature. Comp. Biochem. Physiol. A. Comp. Physiol. 82, 797–803.

Ishida, A.T., Kaneko, A., Tachibana, M., 1984. Responses of solitary retinal horizontal cells from *Carassius auratus* to L-glutamate and related amino acids. J. Physiol. 348, 255–270.

Johansson, D., Nilsson, G.E., Døving, K.B., 1997. Anoxic depression of light-evoked potentials in retina and optic tectum of crucian carp. Neurosci. Lett. 237, 73–76.

Jonz, M.G., Barnes, S., 2007. Proton modulation of ion channels in isolated horizontal cells of the goldfish retina. J. Physiol. 581, 529–541.

Kim, J.P., Koh, J., Choi, D.W., 1987. l-Homocysteate is a potent neurotoxin on cultured cortical neurons. Brain Res. 437, 103–110.

Klaassen, L.J., Sun, Z., Steijaert, M.N., Bolte, P., Fahrenfort, I., Sjoerdsma, T., Klooster, J., Claassen, Y., Shields, C.R., Ten Eikelder, H.M.M., Janssen-Bienhold, U., Zoidl, G., McMahon, D.G., Kamermans, M., 2011. Synaptic transmission from horizontal cells to cones is impaired by loss of connexin hemichannels. PLoS Biol 9(7):e1001107.

Klooster, J., Nunes Cardozo, B., Yazulla, S., Kamermans, M., 2004. Postsynaptic localization of γ-aminobutyric acid transporters and receptors in the outer plexiform layer of the goldfish retina: An ultrastructural study. J. Comp. Neurol. 474, 58–74.

Koh, J., Goldberg, M., Hartley, D., Choi, D., 1990. Non-NMDA receptor-mediated neurotoxicity in cortical culture. J. Neurosci. 10, 693–705.

Koulen, P., Brandstätter, J.H., Kröger, S., Enz, R., Bormann, J., Wässle, H., 1997. Immunocytochemical localization of the GABA(C) receptor rho subunits in the cat, goldfish, and chicken retina. J. Comp. Neurol. 380, 520–532.

Lam, D.M.K., Steinman, L., 1971. The uptake of [γ-^{3}H] aminobutyric acid in the goldfish retina. Proc. Natl. Acad. Sci. USA. 68, 2777-2781.

Linn, C.L., Gafka, A.C., 1999. Activation of metabotropic glutamate receptors modulates the voltage-gated sustained calcium current in a teleost horizontal cell. J. Neurophysiol. 81, 425–434.

Linn, C.L., Gafka, A.C., 2001. Modulation of a voltage-gated calcium channel linked to activation of glutamate receptors and calcium-induced calcium release in the catfish retina. J. Physiol. 535, 47–63.

Linn, C.P., Christensen, B.N., 1992. Excitatory amino acid regulation of intracellular Ca^{2+} in isolated catfish cone horizontal cells measured under voltage- and concentration-clamp conditions. J. Neurosci. 12, 2156–2164.

Lucas, D.R., Newhouse, J.P., 1957. The toxic effect of sodium L-Ggutamate on the inner layers of the retina. Arch. Ophthalmol. 58, 193–201.

Lutz, P.L., McMahon, P., Rosenthal, M., Sick, T.J., 1984. Relationships between aerobic and anaerobic energy production in turtle brain in situ. Am. J. Physiol. Regul. Integr. Comp. Physiol. 247, 740-744.

Lutz, P.L., Nilsson, G.E., 2004. Vertebrate brains at the pilot light. Respir. Physiol. Neurobiol. 141, 285–296.

MacDermott, A.B., Mayer, M.L., Westbrook, G.L., Smith, S.J., Barker, J.L., 1986. NMDA-receptor activation increases cytoplasmic calcium concentration in cultured spinal cord neurones. Nature. 321, 519–522.

Marc, R.E., Stell, W.K., Bok, D., Lam, D.M.K., 1978. GABA-ergic pathways in the goldfish retina. Journal of comparative neurology (1911) 182, 221–245.

Miller, R.F., Dacheux, R.F., 1983. Intracellular chloride in retinal neurons: Measurement and meaning. Vision Res. 23, 399–411.

Minners, J., McLeod, C.J., Sack, M.N., 2003. Mitochondrial plasticity in classical ischemic preconditioning-moving beyond the mitochondrial K_{ATP} channel. Cardiovasc. Res. 59, 1–6.

Montero, M., Alonso, M.T., Albillos, A., García-Sancho, J., Alvarez, J., 2001. Mitochondrial Ca^{2+}-induced Ca $^{2+}$ release mediated by the Ca $^{2+}$ uniporter. Mol. Biol. Cell. 12, 63–71.

Neal, M.J., Cunningham, J.R., Hutson, P.H., Hogg, J., 1994. Effects of ischaemia on neurotransmitter release from the isolated retina. J. Neurochem. 62, 1025–1033.

Nilsson, G.E., 1990. Long-term anoxia in crucian carp: Changes in the levels of amino acid and monoamine neurotransmitters in the brain, catecholamines in chromaffin tissue, and liver glycogen. J. Exp. Biol. 150, 295–320.

Nilsson, G.E., 1992. Evidence for a role of GABA in metabolic depression during anoxia in crucian carp (*Carassius Carassius*). J. Exp. Biol. 164, 243–259.

Nilsson, G.E., Lutz, P.L., 2004. Anoxia Tolerant Brains. J. Cereb. Blood Flow Metab. 24, 475–486.

Nilsson, G.E., Lutz, P.L., 1991. Release of inhibitory neurotransmitters in response to anoxia in turtle brain. Am. J. Physiol. 261, 32–37.

Nilsson, G.E., Rosen, P., Johansson, D., 1993. Anoxic depression of spontaneous locomotor activity in crucian carp quantified by a computerized imaging technique. J. Exp. Biol. 180, 153–162.

Paik, S.S., Park, N.G., Lee, S.J., Han, H.K., Jung, C.S., Bai, S.H., Chun, M.H., 2003. GABA receptors on horizontal cells in the goldfish retina. Vision Res. 43, 2101–2106.

Pamenter, M.E., Hogg, D.W., Ormond, J., Shin, D.S., Woodin, M.A., Buck, L.T., 2011. Endogenous $GABA_A$ and $GABA_B$ receptor-mediated electrical suppression is critical to neuronal anoxia tolerance. Proc. Natl. Acad. Sci. USA. 108, 11274–11279.

Pamenter, M.E., Shin, D.S., Buck, L.T., 2008a. AMPA receptors undergo channel arrest in the anoxic turtle cortex. J. Physiol. 294, 606–613.

Pamenter, M.E., Shin, D.S., Cooray, M., Buck, L.T., 2008b. Mitochondrial ATP-sensitive K^+ channels regulate NMDAR activity in the cortex of the anoxic western painted turtle. J. Physiol. 586, 1043–1058.

Pek-Scott, M., Lutz, P.L., 1998. ATP-sensitive K^+ channel activation provides transient protection to the anoxic turtle brain. Am. J. Physiol. Regul. Integr. Comp. Physiol. 275, 2023-2027.

Perez-Pinzon, M.A., Rosenthal, M., Sick, T.J., Lutz, P.L., Pablo, J., Mash, D., 1992. Downregulation of sodium channels during anoxia: a putative survival strategy of turtle brain. Am. J. Physiol. Regul. Integr. Comp. Physiol. 262, 712-715.

Qian, H., Dowling, J.E., 1993. Novel GABA responses from rod-driven retinal horizontal cells. Nature. 361, 162–164.

Ramón y Cajal, S., 1909. Histologie du système nerveux de l'homme & des vertébrés. Maloine, Paris.

Rodgers-Garlick, C. I., Hogg, D.W., Buck, L.T., 2013. Oxygen-sensitive reduction in Ca^{2+}-activated K^+ channel open probability in turtle cerebrocortex. Neurosci. 237, 243–254.

Schmitz, Y., Witkovsky, P., 1997. Dependence of photoreceptor glutamate release on a dihydropyridine-sensitive calcium channel. Neurosci. 78, 1209–1216.

Schubert, T., Weiler, R., Feigenspan, A., 2006. Intracellular calcium is regulated by different pathways in horizontal cells of the mouse retina. J. Neurophysiol. 96, 1278–1292.

Schwartz, E.A., 2002. Transport-mediated synapses in the retina. Physiol. Rev. 82, 875–891.

Shin, D.S.-H., Wilkie, M.P., Pamenter, M.E., Buck, L.T., 2005. Calcium and protein phosphatase 1/2A attenuate N-methyl-d-aspartate receptor activity in the anoxic turtle cortex. Comp. Biochem. Physiol. A. Mol. Integr. Physiol. 142, 50–57.

Shoubridge, E.A., Hochachka, P.W., 1980. Ethanol: Novel end product of vertebrate anaerobic metabolism. Science. 209, 308–309.

Siman, R., Noszek, J., Kegerise, C., 1989. Calpain I activation is specifically related to excitatory amino acid induction of hippocampal damage. J Neurosci. 9, 1579–1590.

Song, P.I., Matsui, J.I., Dowling, J.E., 2008. Morphological types and connectivity of horizontal cells found in the adult zebrafish (*Danio rerio*) retina. J. Comp. Neurol. 506, 328–338.

Stell, W.K., Lightfoot, D.O., 1975. Color-specific interconnections of cones and horizontal cells in the retina of the goldfish. J. Comp. Neurol. 159, 473–501.

Sterling, P., Matthews, G., 2005. Structure and function of ribbon synapses. Trends Neurosci. 28, 20–29.

Suryanarayanan, A., Slaughter, M.M., 2006. synaptic transmission mediated by internal calcium stores in rod photoreceptors. J. Neurosci. 26, 1759–1766.

Suzue, T., Wu, G.B., Furukawa, T., 1987. High susceptibility to hypoxia of afferent synaptic transmission in the goldfish sacculus. J.Neurophysiol. 58, 1066–1079.

Svaetichin, G., MacNichol Jr, E.F., 1958. Retinal mechanisms for chromic and achromic vision. Ann. N .Y. Acad. Sci. 74, 385–404.

Szydlowska, K., Tymianski, M., 2010. Calcium, ischemia and excitotoxicity. Cell Calcium 47, 122–129.

Tachibana, M., 1981. Membrane properties of solitary horizontal cells isolated from goldfish retina. J. Physiol. 321, 141–161.

Tachibana, M., 1983. Ionic currents of solitary horizontal cells isolated from goldfish retina. J. Physiol. 345, 329–351.

Thoreson, W.B., Babai, N., Bartoletti, T.M., 2008. Feedback from horizontal cells to rod photoreceptors in vertebrate retina. J. Neurosci. 28, 5691–5695.

Thoreson, W.B., Mangel, S.C., 2012. Lateral interactions in the outer retina. Prog. Retin. Eye Res. 31, 407-441.

Tornqvist, K., Yang, X., Dowling, J., 1988. Modulation of cone horizontal cell activity in the teleost fish retina. III. Effects of prolonged darkness and dopamine on electrical coupling between horizontal cells. J Neurosci. 8, 2279–2288.

Twig, G., Levy, H., Perlman, I., 2003. Color opponency in horizontal cells of the vertebrate retina. Prog. Retin. Eye Res. 22, 31–68.

Ultsch, G.R., Jackson, D.C., 1982. Long-term submergence at 3°C of the turtle, *Chrysemys Picta Bellii*, in normoxic and severely hypoxic water. J. Exp. Biol. 96, 11–28.

van Waversveld, J., Addink, A.D.F., van den Thillart, G., 1989. The anaerobic energy metabolism of goldfish determined by simultaneous direct and indirect calorimetry during anoxia and hypoxia. J. Comp. Physiol. 159, 263–268.

Verweij, J., Kamermans, M., Spekreijse, H., 1996. Horizontal cells feed back to cones by shifting the cone calcium-current activation range. Vision Res. 36, 3943–3953.

Vessey, J.P., Stratis, A.K., Daniels, B.A., Da Silva, N., Jonz, M.G., Lalonde, M.R., Baldridge, W.H., Barnes, S., 2005. Proton-mediated feedback inhibition of presynaptic calcium channels at the cone photoreceptor synapse. J. Neurosci. 25, 4108–4117.

Walker, R.M., Johansen, P.H., 1977a. Anaerobic metabolism in goldfish (*Carassius auratus*). Can. J. Zool. 55, 1304–1311.

Walker, R.M., Johansen, P.H., 1977b. Anaerobic metabolism in goldfish (*Carassius auratus*). Can. J. Zool. 55, 1304–1311.

Watkins, J.C., Krogsgaard-Larsen, P., Honoré, T., 1990. Structure-activity relationships in the development of excitatory amino acid receptor agonists and competitive antagonists. Trends Pharmacol. Sci. 11, 25–33.

Watkins, J.C., Olverman, H.J., 1987. Agonists and antagonists for excitatory amino acid receptors. Trends Neurosci. 10, 265–272.

Wilkie, M.P., Pamenter, M.E., Alkabie, S., Carapic, D., Shin, D.S.H., Buck, L.T., 2008. Evidence of anoxia-induced channel arrest in the brain of the goldfish (*Carassius auratus*). Comp. Biochem. Physiol. Toxicol. Pharmacol. 148, 355–362.

Witkovsky, P., Schmitz, Y., Akopian, A., Krizaj, D., Tranchina, D., 1997. Gain of rod to horizontal cell synaptic transfer: Relation to glutamate release and a dihydropyridine-sensitive calcium current. J. Neurosci. 17, 7297–7306.

Wong-Riley, M., 2010. Energy metabolism of the visual system. Eye Brain 2, 99–116.

Yazulla, S., 1985. Evoked efflux of [^{3}H]GABA from goldfish retina in the dark. Brain Res. 325, 171–180.

Young, L.H., Dowling, J.E., 1984. Monoclonal antibodies distinguish subtypes of retinal horizontal cells. Proc. Natl. Acad. Sci. USA 81, 6255–6259.

Zivkovic, G., Buck, L.T., 2010. Regulation of AMPA receptor currents by mitochondrial ATP-sensitive K^+ channels in anoxic turtle neurons. J. Neurophysiol. 104, 1913–1922.